AEDC-TR-76-138

AIRCRAFT MOTION SENSITIVITY TO CROSS AND

CROSS-COUPLING DAMPING DERIVATIVES

PROPULSION WIND TUNNEL FACILITY
ARNOLD ENGINEERING DEVELOPMENT CENTER
AIR FORCE SYSTEMS COMMAND
ARNOLD AIR FORCE STATION, TENNESSEE 37389

November 1976

Final Report for Period 1 July 1975 — 30 June 1976

Prepared for

DIRECTORATE OF TECHNOLOGY
ARNOLD ENGINEERING DEVELOPMENT CENTER
ARNOLD AIR FORCE STATION, TENNESSEE 37389

APPROVAL STATEMENT

This technical report has been reviewed and is approved for publication.

FOR THE COMMANDER

KENNETH B. HARWOOD
Major, CF
Research & Development
  Division
Directorate of Technology

ROBERT O. DIETZ
Director of Technology

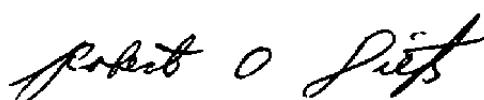| REPORT DOCUMENTATION PAGE		READ INSTRUCTIONS BEFORE COMPLETING FORM
1 REPORT NUMBER AEDC-TR-76-138	2 GOVT ACCESSION NO	3 RECIPIENT'S CATALOG NUMBER
4 TITLE (and Subtitle) AIRCRAFT MOTION SENSITIVITY TO CROSS AND CROSS-COUPLING DAMPING DERIVATIVES		5 TYPE OF REPORT & PERIOD COVERED Final Report, 1 July 1975 - 30 June 1976
		6 PERFORMING ORG REPORT NUMBER
7 AUTHOR(s) R. W. Butler, ARO, Inc.		8 CONTRACT OR GRANT NUMBER(s)
9 PERFORMING ORGANIZATION NAME AND ADDRESS Arnold Engineering Development Center (DY) Air Force Systems Command Arnold Air Force Station, TN 37389		10 PROGRAM ELEMENT PROJECT, TASK AREA & WORK UNIT NUMBERS Program Element 65807F
11 CONTROLLING OFFICE NAME AND ADDRESS Arnold Engineering Development Center (DYFS) Arnold Air Force Station, TN 37389		12 REPORT DATE November 1976
		13 NUMBER OF PAGES 54
14 MONITORING AGENCY NAME & ADDRESS(If different from Controlling Office)		15 SECURITY CLASS. (of this report) UNCLASSIFIED
		15a DECLASSIFICATION DOWNGRADING SCHEDULE N/A
16 DISTRIBUTION STATEMENT (of this Report) Approved for public release; distribution unlimited.		
17 DISTRIBUTION STATEMENT (of the abstract entered in Block 20, if different from Report)		
18 SUPPLEMENTARY NOTES Available in DDC.		

19 KEY WORDS (Continue on reverse side if necessary and identify by block number)

motion	A-7 aircraft
simulation	F-5 aircraft
wind tunnel tests	captive tests
F-4 aircraft	

20 ABSTRACT (Continue on reverse side if necessary and identify by block number)

An investigation was conducted to provide some insight into the importance of dynamic cross and cross-coupling derivatives in motion simulation studies of fighter aircraft in the maneuvering flight regime. The aircraft motion sensitivity to the various derivatives is ascertained in level and turning flight utilizing a 5 deg of freedom linearized stability program. The results are presented in a root locus format. The results of the study show

DD FORM 1473 EDITION OF 1 NOV 65 IS OBSOLETE
1 JAN 73

20. ABSTRACT (Continued)

that, in the flight regime examined, the dynamic cross derivatives C_{n_p}, C_{ℓ_r}, and $C_{\ell_{\dot{\beta}}}$ and the $\dot{\beta}$ derivative $C_{n_{\dot{\beta}}}$ may significantly alter the stability characteristics of the F-4, A-7, and F-5 aircraft and therefore should be considered in motion simulation studies of these aircraft. Likewise, the study indicates that the dynamic cross-coupling derivatives C_{ℓ_q}, C_{n_q}, C_{m_p}, C_{m_r}, $C_{\ell_{\dot{\alpha}}}$, and $C_{n_{\dot{\alpha}}}$ have little or no effect on the stability modes of the above aircraft; these derivatives are therefore considered unimportant in motion simulation of the aircraft in the maneuvering flight regime.

PREFACE

The work reported herein was conducted by the Arnold Engineering Development Center (AEDC), Air Force Systems Command (AFSC), under Program Element 65807F. The results of the research were obtained by ARO, Inc. (a subsidiary of Sverdrup & Parcel and Associates, Inc.), contract operator of AEDC, AFSC, Arnold Air Force Station, Tennessee, under ARO Project Number P33A-C5A. The author of this report was R. W. Butler, ARO, Inc. Analysis of the data was completed on May 31, 1976, and the manuscript (ARO Control No. ARO-PWT-TR-76-88) was submitted for publication on August 11, 1976.

CONTENTS

ILLUSTRATIONS

Figure

TABLES

APPENDIX

1.0 INTRODUCTION

Renewed interest in departure characteristics of high performance military aircraft over the past decade has resulted in the development of a captive aircraft departure system (CADS) testing technique at the Arnold Engineering Development Center (AEDC). The CADS testing technique (Ref. 1) is capable of generating aircraft maneuvers up to and including departure in the wind tunnel utilizing the tunnel as an analog forcing function. Aircraft static external forces and moments required in the computer simulation are measured during the course of the maneuver with all dynamic components being input parameters. In the past, when aircraft operating envelopes were in the linear aerodynamic (low angle-of-attack) flight regime these dynamic components consisted primarily of direct and cross-damping derivatives. At the high angle-of-attack, severe maneuvering conditions of modern fighter aircraft, there is reason to believe that additional dynamic derivatives (cross coupling) may be needed to insure accurate motion simulation. This assumption is based on work reported by Orlik-Ruckemann and others in Ref. 2. Experimental data in Ref. 2 indicate that at high angles of attack (maneuvering flight condition) both cross and cross-coupling dynamic derivatives acquire values orders of magnitude larger than those at the lower angles (cruise flight condition). The subject report investigates the effect of these large values in cross and cross-coupling derivatives on aircraft motion and thereby identifies the important dynamic derivatives to be included in the CADS and similar motion simulation studies.

Aircraft motion consists of combinations of the basic longitudinal and lateral directional characteristic modes of motion. The sensitivity of each of these characteristic modes to variations in the dynamic derivatives is an indicator of the derivatives which should be included in motion simulation studies. A 5 deg of freedom (5-DOF) linearized stability program is utilized in this report for identifying mode changes with variations in derivatives. The linearized program identifies the basic aircraft modes with the exception of the longitudinal phugoid. Simplifying assumptions used in linearizing the program required that the aircraft velocity remain constant, thereby eliminating the phugoid mode. To simulate maneuvering flight, the linearized analysis is performed in both level and turning flight. Changes in the motion modes with derivative variations are depicted in root locus diagrams. Three typical fighter aircraft configurations are investigated in the analysis, the F-4, A-7, and F-5 aircraft. These aircraft were chosen because each is characterized by distinct flying qualities which represent areas of interest in flight dynamics of modern high performance military aircraft. In addition to the above cross and cross-coupling derivative investigation, the importance of the direct acceleration derivative, $C_{n_{\dot{\beta}}}$, in high angle-of-attack motion simulation is reviewed.

2.0 BACKGROUND

Aircraft dynamic damping derivatives are normally categorized into three distinct groups: direct, cross, and cross-coupling. The primary derivatives associated with each of these groups are shown in Fig. 1. At low angles of attack, which are characteristic of aircraft cruise flight conditions, the dynamic cross and cross-coupling derivatives can be predicted analytically (Refs. 3 through 6). Calculations using the prediction techniques normally produce quite accurate results in both longitudinal and lateral directional derivatives (Ref. 7). These derivatives normally exhibit small variations with changes in flight conditions at low angles of attack, thereby producing a small constant effect on the aircraft flight characteristics. As a result, derivatives are often input to motion simulation programs as constant values with good success. Both calculated and measured values of the cross-coupling derivatives in this flight regime are small and are normally omitted from the motion simulation.

On the other hand, the flight envelope of the current generation of fighter aircraft necessitates improved prediction and motion simulation techniques because of the aircraft's greatly expanded operational envelope. The high angle of attack and high speeds at which these aircraft operate produce nonlinear aerodynamic flow phenomena such as separated flows, vortex shedding, etc. Not only these phenomena, but also certain asymmetric flows such as separation on the leeward wing or vortex shedding from the aircraft forebody, which can occur at high angles of sideslip, all have a significant influence on the aircraft dynamic derivatives. The cross-coupling derivatives previously considered to have values near zero assume values which are 10 to 15 percent of the cross derivatives on current fighter configurations (Ref. 2). The cross and cross-coupling derivatives not only increase in magnitude but often experience sign changes over very small angle-of-attack ranges. Because of these effects, all dynamic derivatives may be required inputs in motion simulation programs as variables, normally functions of angle of attack and angle of sideslip.

All derivatives listed in Fig. 1 may not be required for achieving accurate motion simulation. The direct damping derivatives are always considered of primary importance and are included in motion simulation studies at low and high angles of attack. This report addresses the importance of the remaining cross and cross-coupling derivatives at high angles of attack.

3.0 AIRCRAFT CONFIGURATIONS

Three aircraft configurations were chosen for this dynamic sensitivity study. Each aircraft was selected on the basis of inherent high angle-of-attack lateral-directional flight characteristics. The intent was to select aircraft which would exhibit a range of

lateral-directional stability characteristics typical of current high performance military aircraft. On the basis of these criteria, configurations similar to the F-4, A-7, and F-5 aircraft were selected for the analysis.

The F-4 configuration, a twin-jet, swept-wing fighter aircraft, is shown in Fig. 2. This configuration possesses a "wing rock" or dutch roll oscillation at high angles of attack (Refs. 8 and 9). As angle of attack increases up to approximately 23 deg, the dutch roll oscillation becomes unstable, resulting in aircraft directional divergence.

The A-7 configuration, a single-engine, swept-wing aircraft, is shown in Fig. 3. This configuration exhibits some directional instability at angles of attack above 20 deg while still possessing lateral stability (Refs. 9 and 10). The A-7 departure is characterized by an abrupt "nose slice".

The F-5 configuration, a twin-engine, tapered-wing aircraft, is shown in Fig. 4. This configuration exhibits excellent lateral-directional dynamic stability characteristics at angles of attack well above that required for wing stall (Ref. 11). The wing-rock and nose-slice phenomena experienced by the F-4 and A-7 configurations are not experienced in the F-5 configuration.

4.0 METHOD OF ANALYSIS

The sensitivity of aircraft motion to variations in aerodynamic and physical characteristics is reflected in its longitudinal and lateral-directional stability modes, the two longitudinal modes being short period and, phugoid, and the three lateral-directional modes being roll, spiral, and dutch roll. These characteristic modes are normally investigated independently through linearized 3 deg of freedom (3-DOF) stability programs. Such programs provide the damping and frequency characteristics of the modes with the aircraft in level flight, with zero angular rates of motion. However, the flight regimes addressed in this report consider both level and turning flight and therefore cannot be correctly investigated with only the 3-DOF program. In addition, the longitudinal and lateral-directional flight modes are separate in the 3-DOF analysis; therefore, the cross-coupling dynamic derivatives are nonexistent in the separated modes.

A 5-DOF linearized stability program has been developed for conducting the dynamic sensitivity study. In this program, the reference flight condition is generalized to include the effect of non-zero bank angle, pitch rate, and yaw rate. The result is a weak coupling between longitudinal and lateral-directional dynamics providing the mechanism for investigating the importance of the cross-coupling dynamic derivatives in turning flight. The 5-DOF system was obtained by eliminating the X-body axis translation equation from the six Euler equations of motion. Omitting this equation requires that the

aircraft remain at a constant velocity along the X axis, thereby alleviating the longitudinal phugoid mode of motion. The lineraized equations of motion derived with these criteria are listed below. The linearization process used is presented in Refs. 3 and 4.

$$\dot{a} - Z_w a - q + \left(g/U_o \sin \phi_o\right)\phi = 0 \tag{1}$$

$$\dot{\beta} - Y_v \beta + \left(\cos \alpha_o - \frac{Y_r}{V_\infty}\right)r - \left(\sin \alpha_o + \frac{Y_p}{V_\infty}\right)'p - \left(\frac{g}{V_\infty} \cos \phi_o\right)\phi = 0 \tag{2}$$

$$\dot{p} - \left(L_p + q_o \frac{I_{xz}}{I_{xx}}\right)p - \frac{I_{xz}}{I_{xx}}\dot{r} + \left(c_1 q_o - L_r\right)r + \left(r_o c_1 - L_q\right)q$$
$$- L_\beta \beta - L_{\dot\beta}\dot\beta - L_{\dot a}\dot{a} = 0 \tag{3}$$

$$\dot{q} - M_q q - \left(2r_o \frac{I_{xz}}{I_{yy}} + M_r\right)r + \left(r_o c_2 - M_p\right)p - M_a a - M_{\dot a}\dot{a} = 0 \tag{4}$$

$$\dot{r} + \left(q_o \frac{I_{xz}}{I_{zz}} - N_r\right)r - \frac{I_{xz}}{I_{zz}}\dot{p} + \left(q_o c_3 - N_p\right)p + \left(r_o \frac{I_{xz}}{I_{zz}} - N_q\right)q$$
$$- N_{\dot\beta}\dot\beta - N_\beta \beta - N_{\dot a}\dot{a} = 0 \tag{5}$$

$$\dot{\theta} - \cos \phi_o q + \sin \phi_o r + \dot\psi_o \phi = 0 \tag{6}$$

$$\dot{\phi} - p - \dot\psi_o \theta = 0 \tag{7}$$

where

$$c_1 = \frac{I_{zz} - I_{yy}}{I_{xx}} \qquad c_2 = \frac{I_{xx} - I_{zz}}{I_{yy}} \qquad c_3 = \frac{I_{yy} - I_{xx}}{I_{zz}}$$

Equations (1) and (2) are the force equations; (3), (4), and (5) are the moment equations; and (6) and (7) the kinematic equations which the motion must satisfy. Initial

pitch attitude and initial roll rate are assumed to be small in the derivation. The equations are referenced to the Eulerian body axis system with the axes' origin at the aircraft center of gravity. The aircraft XZ plane is the plane of symmetry.

Initial inputs ϕ_0, $\dot{\psi}_0$, q_0, and r_0, required for solving the equations, are evaluated from the conditions for steady, turning flight.

$$\dot{\psi}_0 = \frac{n \sin \phi_0}{V_\infty} g \tag{8}$$

$$q_0 = \dot{\psi}_0 \sin \phi_0 \tag{9}$$

$$r_0 = \dot{\psi}_0 \cos \phi_0 \tag{10}$$

By applying the Laplace operator, one obtains the 7 x 7 characteristic determinant shown in Appendix A. Values e_1 through e_{14} of the determinant correspond to terms in parentheses in the respective equations (1) through (7). Solving this determinant yields the characteristics equation below, with coefficients also defined in Appendix A.

$$
\begin{aligned}
C_{11}\lambda^7 &- AC1\lambda^6 + (AC2 + AB1 - \dot{\psi}_0^2 C_{11})\lambda^5 + (AB2 - AC3 + \dot{\psi}_0 AD1 + AE1\dot{\psi}_0 \\
&+ \dot{\psi}_0^2 AC1)\lambda^4 + (AB3 + AC4 + \dot{\psi}_0 AD2 - \dot{\psi}_0 AE2 + \dot{\psi}_0 AC2)\lambda^3 \\
&+ (AB4 - AC5 + \dot{\psi}_0 AD3 + \dot{\psi}_0 AE3 - \dot{\psi}_0^2 AC3)\lambda^2 \\
&+ (AB5 + \dot{\psi}_0 AD4 - \dot{\psi}_0 AE4 + \dot{\psi}_0^2 AC1)\lambda \\
&+ (\dot{\psi}_0 AD5 + \dot{\psi}_0 AE5 + \dot{\psi}_0^2 AC5) = 0 \tag{11}
\end{aligned}
$$

This algebraic expression for the characteristic determinant (Appendix A) was formulated for use in future work of generating aircraft stability boundaries by utilizing the Taylor series expansion technique of Ref. 12

With the seventh-order characteristic equation, three new eigenvalues appear in addition to those which normally occur with a 3-DOF lateral-directional system. Two of the eigenvalues represent the longitudinal short period mode, and the third eigenvalue represents a coupling with the lateral-directional spiral mode to form an oscillatory spiral. The remaining lateral-directional modes are the conventional dutch roll and the roll.

5.0 RESULTS AND DISCUSSION

5.1 GENERAL

The aerodynamic and physical characteristics for each of the aircraft configurations evaluated are presented in Tables 1, 2, and 3.

The F-4 characteristics are given in Table 1. The mass, inertia, and geometric parameters shown represent a clean F-4 configuration as outlined in Refs. 7, 13, and 14. The aerodynamic static and dynamic stability derivatives were acquired from Refs. 7 and 13. The longitudinal and lateral-directional derivatives were obtained over angle-of-attack and angle-of-sideslip ranges, respectively, of ±5 deg about the aircraft trim angle of attack of 29 deg. The trim angle of attack represents the maximum trim capability of the horizontal tail (i_t = -25) based on static force tests.

The A-7 characteristics are shown in Table 2. The mass, inertia, and geometric parameters are for a clean aircraft configuration (Ref. 15). All aerodynamic characteristics are from unpublished static wind tunnel data. Static derivatives were calculated over angle-of-attack and angle-of-sideslip ranges of ±5 deg about a nominal trim angle of attack of 26.5 deg. The 26.5-deg attack angle corresponds to a maximum horizontal stabilizer setting of -25 deg (i_t = -25).

The F-5 aerodynamic characteristics are shown in Table 3. Mass, inertia, and geometric characteristics are representative of those for the clean F-5E aircraft. All aerodynamic characteristics were acquired from wind tunnel data presented in Ref. 11. Both static and dynamic derivatives were evaluated about an angle of attack of 28 deg with static derivative calculations being over a ±5-deg range. The 28-deg angle of attack corresponds to an unrealistic horizontal stabilizer setting of -25 deg (i_t = -25). Maximum horizontal stabilizer deflection on the F-5 aircraft is -17 deg. The increased deflection was used to produce higher angles of attack representative of flight at load factors greater than 1g.

The dynamic stability analysis on all three aircraft was conducted in 1-g (level), 3-g (turning), and 6-g (turning) flight at an altitude of 30,000 ft. The turning flight conditions simulate the aircraft in the maneuvering flight regime. To isolate the effects of the longitudinal and lateral-directional coupling, which occur in turning flight, on the dynamic sensitivity study, it was deemed necessary to maintain identical aerodynamic stability derivatives at all three flight conditions. This was accomplished by maintaining a constant angle of attack at all flight conditions. The aircraft airspeed was adjusted to achieve the desired load factor and maintain a constant altitude. It was assumed that the aerodynamic coefficients do not change significantly over the speed ranges encountered.

A summary of the flight conditions for simulating the aircraft/flight combinations utilized is given in Table 4.

5.2 DYNAMIC CROSS DERIVATIVE AND $C_{n_{\dot{\beta}}}$ VARIATIONS

Fighter aircraft motion sensitivity to variations in the dynamic cross derivatives C_{ℓ_r}, C_{n_p}, and $C_{\ell_{\dot{\beta}}}$ is shown in Figs. 5, 6, and 7, respectively. Each figure represents changes in the F-4, A-7, and F-5 aircraft longitudinal and lateral-directional modes of flight with variations in the dynamic cross derivatives. As noted previously, the longitudinal phugoid motion is not included. Each cross derivative is varied over a range of ±5 per radian, a variation which, in most cases, is an order of magnitude greater than that nominally experienced by fighter-type aircraft. As the derivatives are varied, the resultant eigenvalues of the characteristic equation are plotted in the root locus format shown (real and imaginary axes representing damping and frequency, respectively). The time required for each mode to damp to one half or diverge to twice amplitude is shown horizontally below each plot with the motion period being shown vertically.

The longitudinal and lateral-directional stability modes of each aircraft are presented for 1-g level and 3-g and 6-g turning flight. In all cases, the motion sensitivity to C_{ℓ_r}, C_{n_p}, and $C_{\ell_{\dot{\beta}}}$ variations increased with the increasing load factor or, in this case, the steady-state turn rate.

When transitioning from level to turning flight the aircraft spiral mode becomes oscillatory. The additional eigenvalue causing the oscillatory spiral results from the non-zero turning rate ($\dot{\psi}_o$) term in the characteristic equation [Eq. (11)]. With zero $\dot{\psi}_o$, Eq. (11) is sixth order and the spiral mode uncoupled. The last two coefficients of Eq. (11) represent the spiral flight mode. The total absence of the F-5 spiral mode in level flight results from a combination of zero $\dot{\psi}_o$, C_{n_r}, and C_{ℓ_p} terms. These zero terms cause the last two coefficients of Eq. (11) to vanish, resulting in the fifth-order characteristic equation. Zero values of C_{ℓ_p} and C_{n_r} correspond to measured damping derivatives (Ref. 11) occurring at the trim flight condition selected (Table 3).

Yaw Rate Parameter - Both F-4 and A-7 roll and dutch roll modes of flight (Fig. 5) show sensitivity to variations in the rolling moment cuased by yaw rate parameter C_{ℓ_r}. The dutch roll mode of the F-4 goes from a divergent oscillation with positive values of C_{ℓ_r} to an aperiodic and finally roll-coupled mode at negative values. The roll and dutch roll modes of the A-7 may be highly divergent or stable, depending on the magnitude and sign of C_{ℓ_r}. The F-5 stability modes show virtually no sensitivity to C_{ℓ_r} variations.

Roll Rate Parameter - Variations of aircraft yawing moment caused by roll rate parameter C_{n_p} affect damping of the F-4, A-7, and F-5 dutch roll and roll modes of

11

flight significantly, as seen in Fig. 6. The longitudinal short period mode of the F-4 also shows a reduction in damping approaching divergence as C_{n_p} becomes more negative. For most aircraft, the more negative C_{n_p} is, the greater is the reduction in dutch roll damping. This trend exists in the A-7 and F-5 aircraft, but not in the F-4, where the dutch roll mode actually becomes stable for values of C_{n_p} less than approximately -2.

Dynamic Stability Derivatives - When wind tunnel testing is employed for generating dynamic stability derivatives, the $C_{\ell_{\dot{\beta}}}$ and $C_{n_{\dot{\beta}}}$ terms are normally coupled with the C_{ℓ_r} and C_{n_r} terms, respectively, in the data acquisition. As a result, motion simulation programs often combine these terms as $(C_{\ell_r} + C_{\ell_{\dot{\beta}}})$ and $(C_{n_r} + C_{n_{\dot{\beta}}})$ and operate on them with the angular rate term r. This technique assumes the predominant term in the expressions to be C_{ℓ_r} and C_{n_r}. Recent experimental data (Ref. 16) have shown fallacies in this assumption during operation at high angles of attack. At high angles of attack, the $C_{\ell_{\dot{\beta}}}$ and $C_{n_{\dot{\beta}}}$ terms become predominant, with the C_{ℓ_r} and C_{n_r} terms approaching zero. The effects that large positive and negative values of $C_{\ell_{\dot{\beta}}}$ and $C_{n_{\dot{\beta}}}$ may have on fighter aircraft stability are shown in Figs. 7 and 8, respectively. Damping of both the F-4 roll and the aperiodic dutch roll roots of Fig. 7 is sensitive to positive and negative variations in $C_{\ell_{\dot{\beta}}}$. The dutch roll mode of tha A-7 aircraft experiences changes in both frequency and damping with $C_{\ell_{\dot{\beta}}}$ variations. As $C_{\ell_{\dot{\beta}}}$ appraoches 2, the mode frequency approaches zero and motion becomes aperiodic. The F-5 dutch roll motion experiences large changes in damping and frequency with $C_{\ell_{\dot{\beta}}}$ variations. The remaining modes of the F-5 are all insensitive to $C_{\ell_{\dot{\beta}}}$ variations.

Root movements identical to those experienced in Fig. 7 are seen in the $C_{n_{\dot{\beta}}}$ variation of Fig. 8. The sensitivity of the F-4, A-7, and F-5 lateral-directional stability modes to variations of $C_{n_{\dot{\beta}}}$ is not as great as that seen in the $C_{\ell_{\dot{\beta}}}$ variation of Fig. 7 but is still of a magnitude to be considered in motion simulation work.

5.3 DYNAMIC CROSS-COUPLING DERIVATIVE VARIATIONS

The dynamic cross-coupling derivatives investigated in this analysis are C_{m_p}, C_{m_r}, $C_{\ell_{\dot{\alpha}}}$, $C_{n_{\dot{\alpha}}}$, C_{n_q}, and C_{ℓ_q}. Sensitivity of the F-4, A-7, and F-5 longitudinal and lateral-directional stability modes to variations of these derivatives over ranges of ±1 per radian are presented in Figs. 9, 10, and 11. The range over which the derivatives are varied was selected from experimental wind tunnel data obtained with an airplane-type configuration (Ref. 2). In all cases, the derivative range employed is more than an order of magnitude, and in most cases, two orders of magnitude, larger than the range exhibited by the experimental data.

C_{m_p}, C_{m_r}, $C_{\ell_{\dot{\alpha}}}$, $C_{n_{\dot{\alpha}}}$ - The group of derivatives shown in Fig. 9 all have one thing in common; they have no effect on the F-4, A-7, and F-5 longitudinal and lateral-directional

stability modes in either level or turning flight. Based on these results, the derivatives should not be required for acquiring accurate motion simulation of fighter aircraft in the maneuvering flight regime.

C_{n_q}, C_{ℓ_q} - Changes occurring in the F-4, A-7, and F-5 stability modes with varying C_{n_q} and C_{ℓ_q} are presented in Figs. 10 and 11, respectively. These derivatives are separated from the above cross-coupling derivatives because they do produce small changes in some of the aircraft stability roots. The greatest root change occurs in the F-4 spiral and dutch roll modes with varying C_{ℓ_q}. Because C_{ℓ_q} was varied over a range (-1, 1) which is approximately two orders of magnitude greater than its nominal value (Ref. 2), the change in the stability roots is considered insignificant.

6.0 CONCLUDING REMARKS

As a result of this analysis, the following observations and conclusions are offered:

1. A 5 deg of freedom linearized stability program provides a technique for investigating lateral-directional stability modes of an aircraft in level and turning flight with light longitudinal coupling.

2. When ascertaining the importance of a dynamic derivative in aircraft stability calculations, one should examine a number of different aircraft configurations; even so, a general conclusion may be impossible.

3. In the 5 deg of freedom linearized analysis, the aircraft stability modes become more sensitive to derivative variations as the load factor or turning rate of the aircraft increases.

4. The dynamic cross derivatives C_{n_p}, C_{ℓ_r}, and $C_{\ell_{\dot\beta}}$ should be included in motion simulation of fighter aircraft examined in the subject analysis.

5. All cross-coupling derivatives C_{ℓ_q}, C_{n_q}, C_{m_p}, C_{m_r}, $C_{\ell_{\dot\alpha}}$, and $C_{n_{\dot\alpha}}$ are considered unimportant in motion simulation of all fighter aircraft examined in this analysis.

6. The rate of change of sideslip derivatives $C_{\ell_{\dot\beta}}$ and $C_{n_{\dot\beta}}$ produces, in each case, significant changes in the lateral-directional stability modes of the aircraft examined. Uncoupling of the $(C_{\ell_r} + C_{\ell_{\dot\beta}})$ and $(C_{n_r} + C_{n_{\dot\beta}})$ terms may be necessary for accurate aircraft motion simulation during operation at high angles of attack.

REFERENCES

1. Butler, R. W. "A Wind Tunnel Captive Aircraft Testing Technique." AEDC-TR-76-22 (ADA023690), April 1976.

2. Orlik-Ruckemann, K. J., Laberge, J. G., and Hanff, E. S. "Measurement of Dynamic Cross-Derivatives Due to Pitching and Yawing." AIAA Paper No. 74-611, July 1974.

3. Etkin, Bernard. "Dynamics of Flight: Stability and Control." John Wiley & Sons, Inc., New York, 1959.

4. Perkins, Courtland D. and Hage, Robert E. "Airplane Performance Stability and Control." John Wiley & Sons, Inc., New York, 1949.

5. Seckel, Edward. "Stability and Control of Airplanes and Helicopters." Academic Press, Inc., New York, 1964.

6. Campbell, John P. and McKinney, Marion O. "Summary of Methods for Calculating Dynamic Lateral Stability and Response and for Estimating Lateral Stability Derivatives." NACA Rep. 1098, 1952.

7. Fletcher, Herman S. "Comparison of Several Methods for Estimating Low-Speed Stability Derivatives for Two Airplane Configurations." NASA TN D-6531, November 1971.

8. Chambers, Joseph R. and Anglin, Ernie L. "Analysis of Lateral-Directional Stability Characteristics of a Twin-Jet Fighter Airplane at High Angles of Attack." NASA TN D-5361, August 1969.

9. Greer, Douglas H. "Summary of Directional Divergence Characteristics of Several High-Performance Aircraft Configurations." NASA TN D-6993, November 1972.

10. Burris, William R. and Hutchins, Dale E. "Effect of Wing Leading Edge Geometry on Maneuvering Boundaries and Stall Departure." AIAA Paper No. 70-904, July 1970.

11. Grafton, Sue B. and Chambers, Joseph R. "Wind-Tunnel Free-Flight Investigation of a Model of a Spin-Resistant Fighter Configuration." NASA TN D-7716, June 1974.

12. Taylor, James L. "A Technique for Mapping Aircraft Stability Boundaries." AEDC-TR-75-46 (ADA010492), May 1975.

13. Grafton, Sue B. and Libbey, Charles E. "Dynamic Stability Derivatives of a Twin-Jet Fighter Model for Angles of Attack from -10° to 110°." NASA TN D-6091, January 1971.

14. Rutan, E. L., McElroy, C. E., and Gentry, J. R. "Stall/Near Stall Investigation of the F-4E Aircraft." FTC-TR-70-20, August 1970.

15. Butler, R. W. "Evaluation of a Wind Tunnel Technique to Determine Aircraft Departure Characteristics." AEDC-TR-73-183 (AD776317), March 1974.

16. Coe, Paul L., Graham, Bruce A., and Chambers, Joseph R. "Summary of Information of Low-Speed Lateral-Directional Derivatives Due to Rate of Change of Sideslip β." NASA TN D-7972, September 1975.

Figure 1. Aircraft damping derivatives.
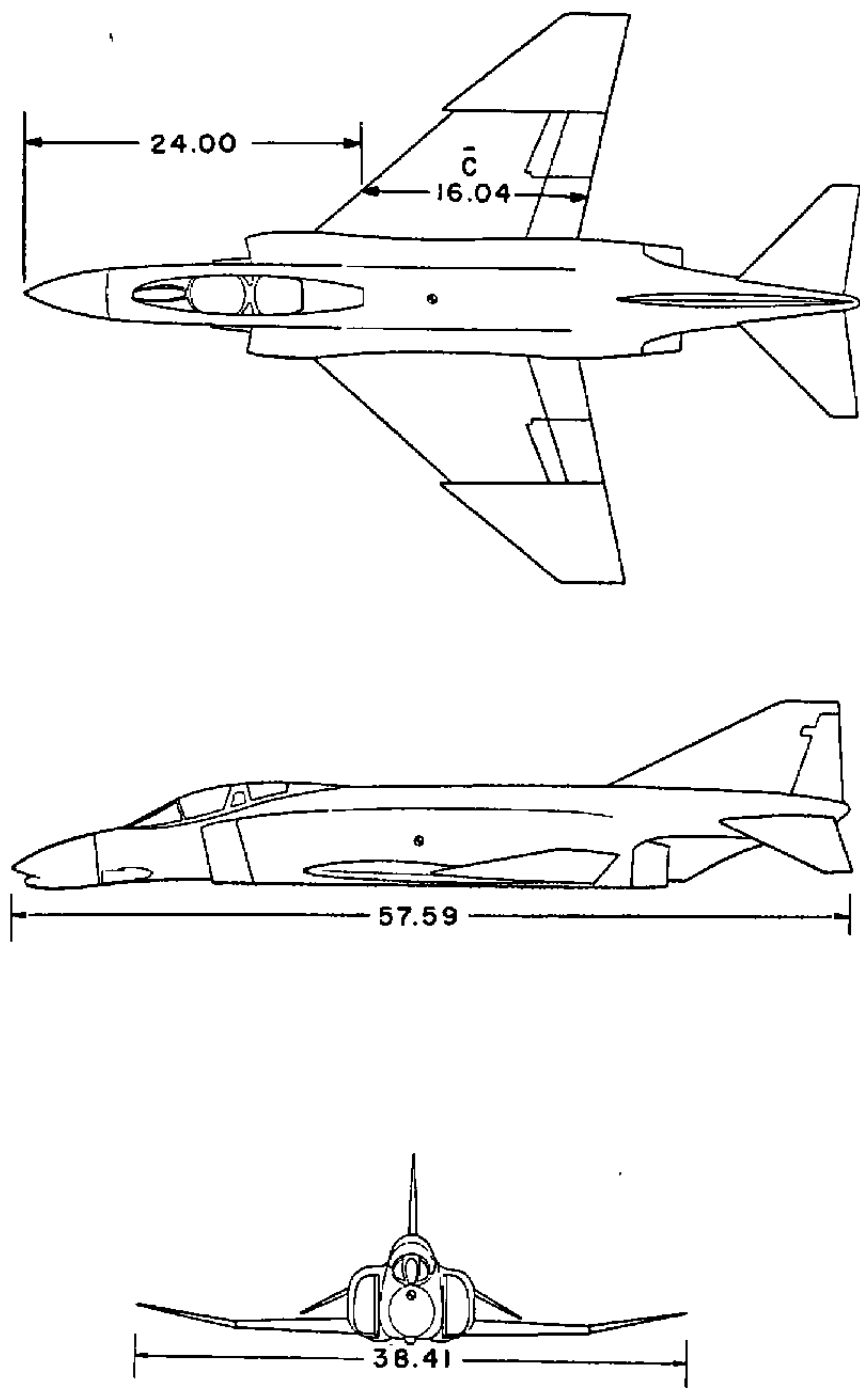
DIMENSIONS IN FEET

Figure 2. Three-view sketch of the F-4 aircraft.
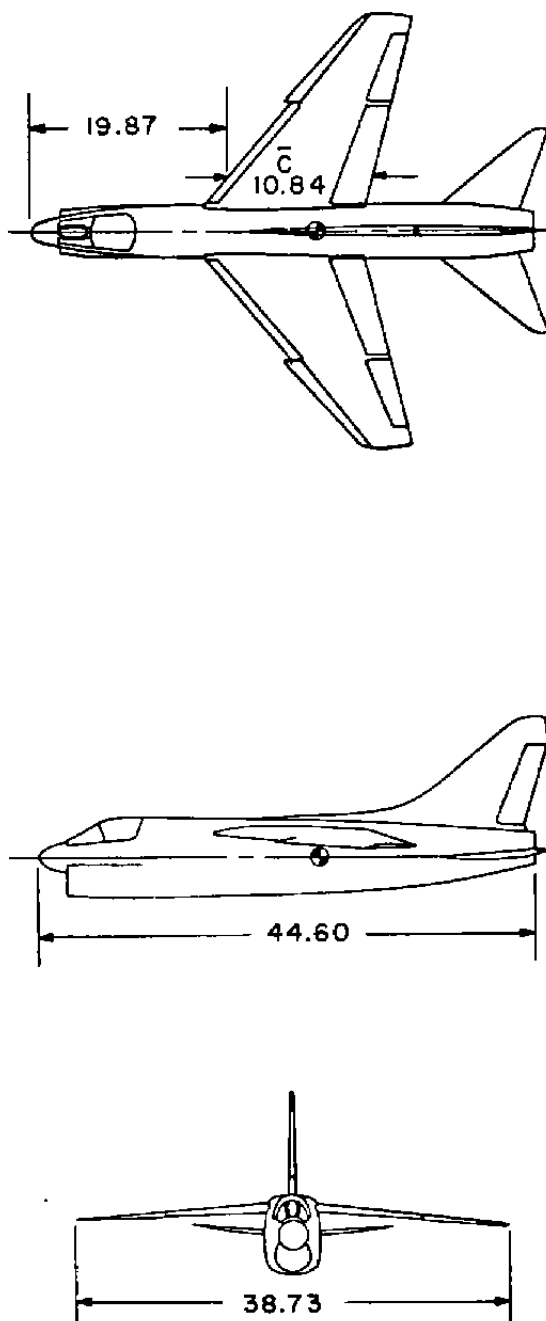
DIMENSIONS IN FEET

Figure 3. Three-view sketch of the A-7 aircraft.
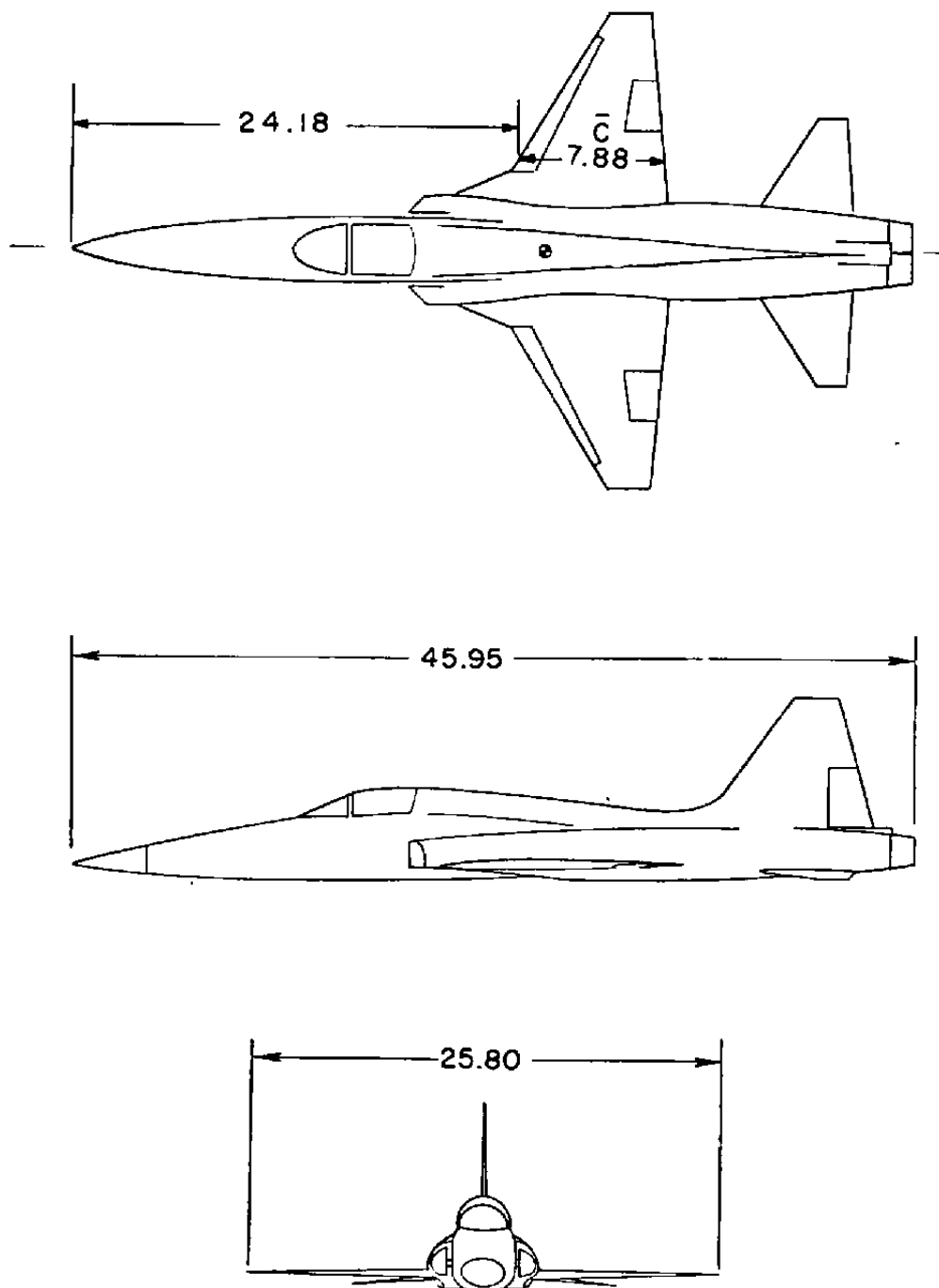
Figure 4. Three-view sketch of the F-5 aircraft.

DIMENSIONS IN FEET
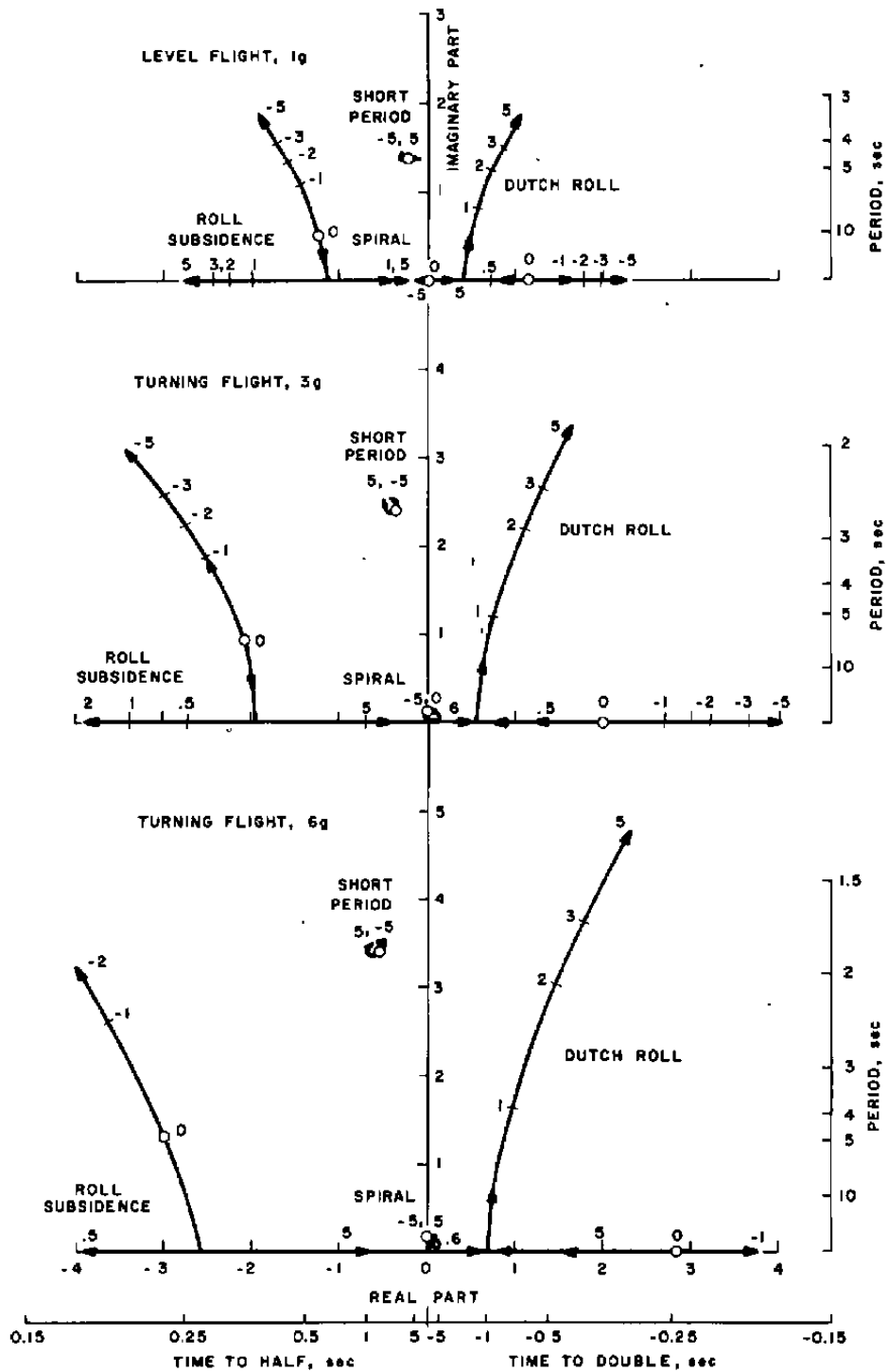
a. F-4

Figure 5. Locus of roots with C_{l_r} variation.
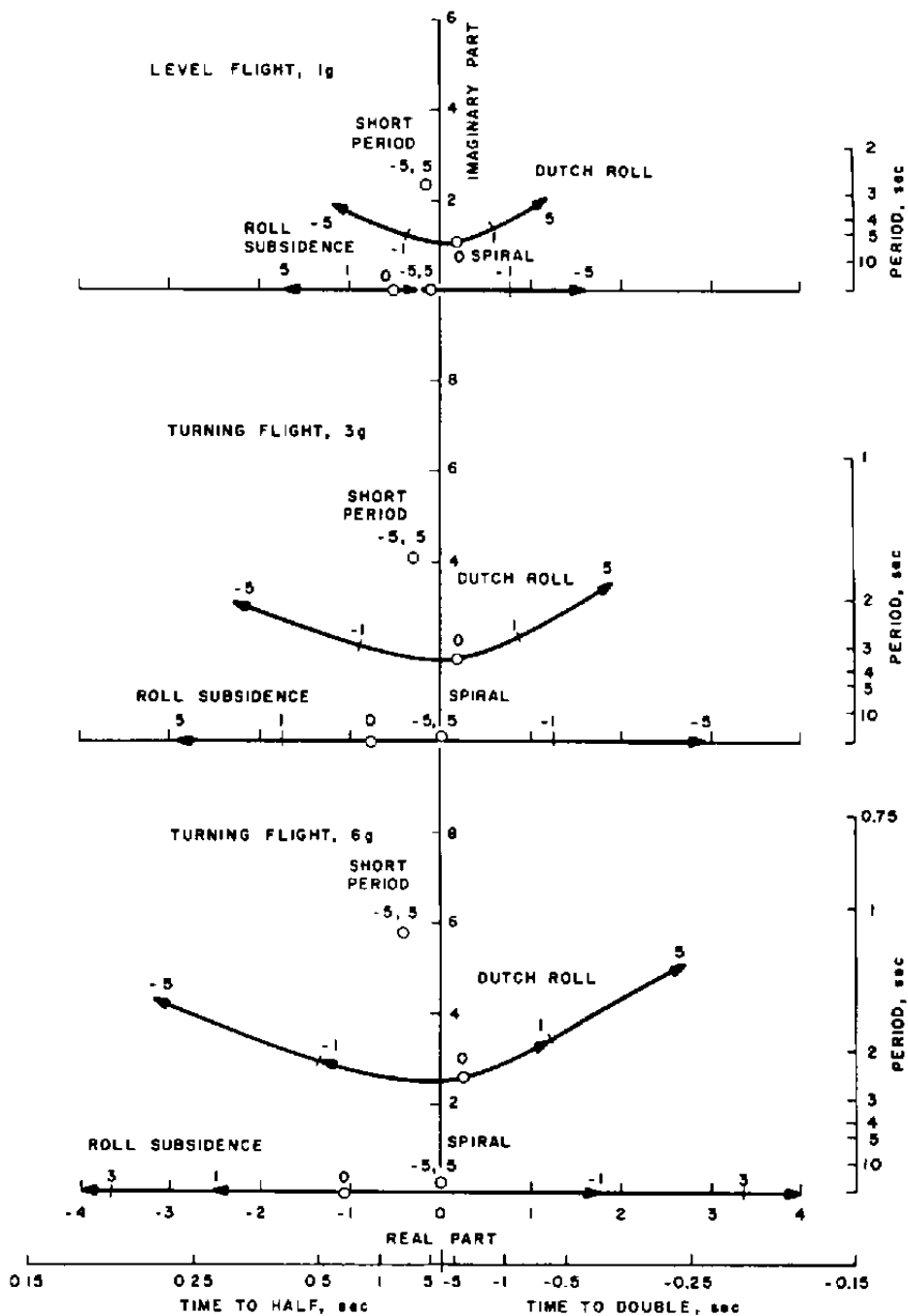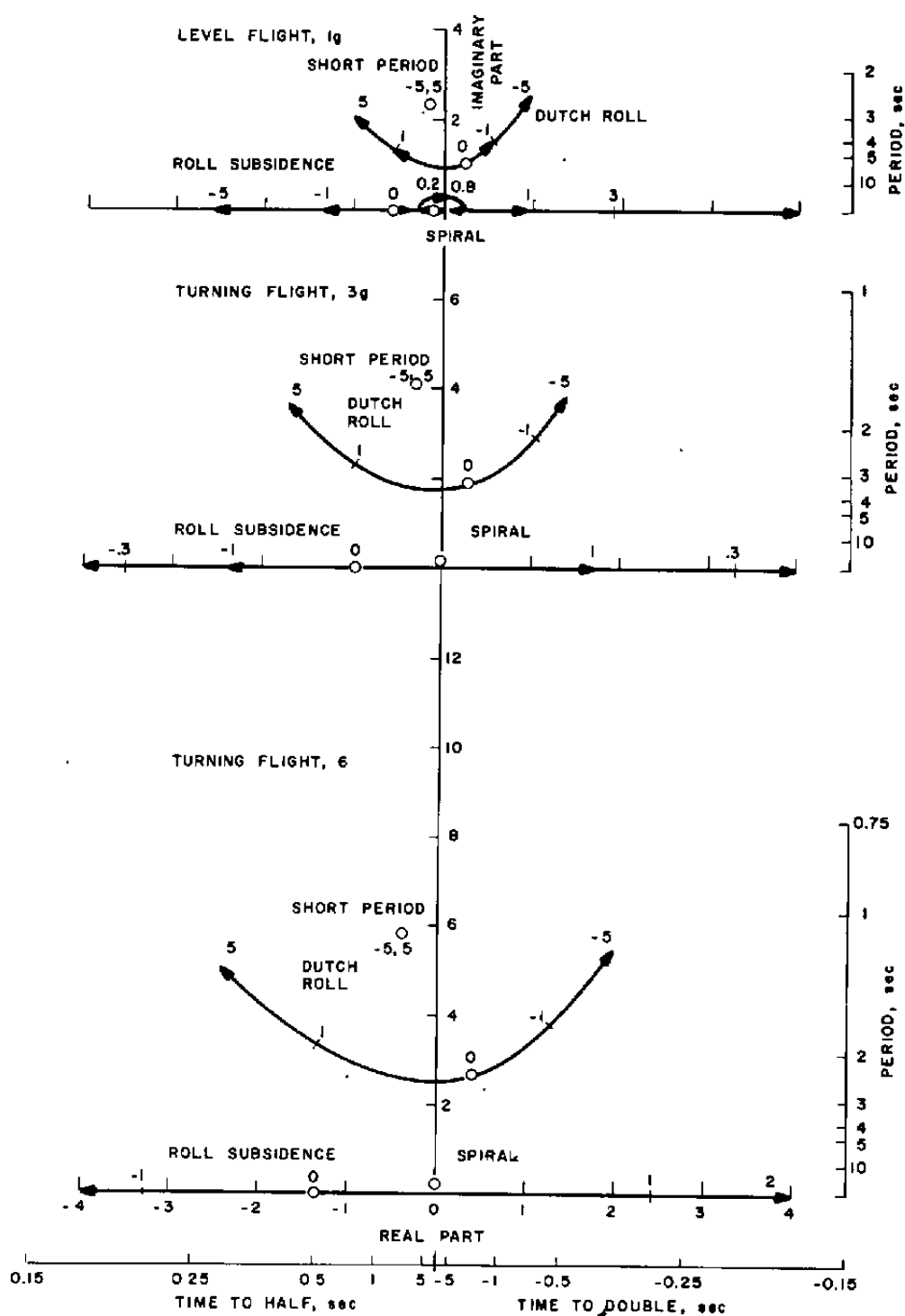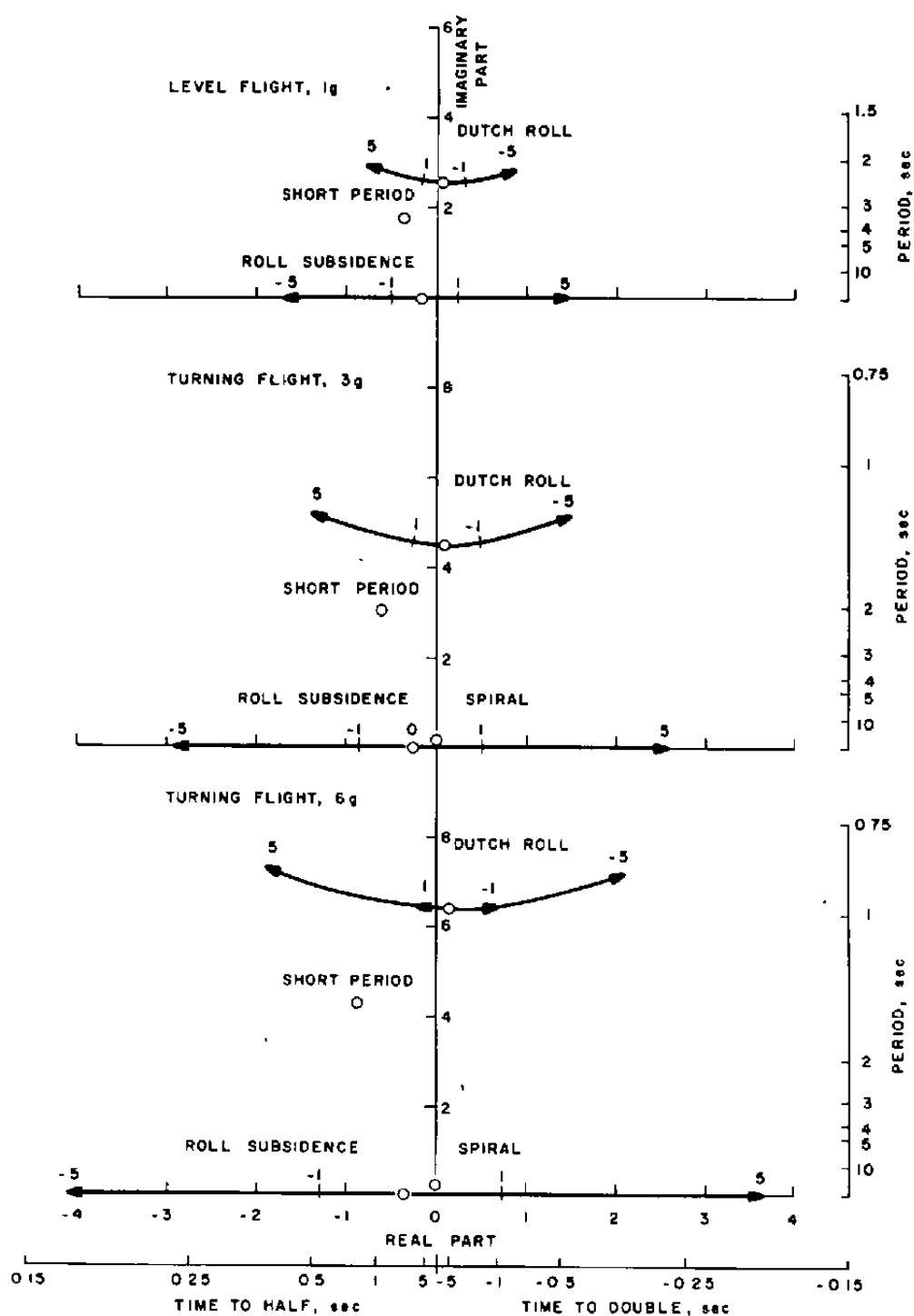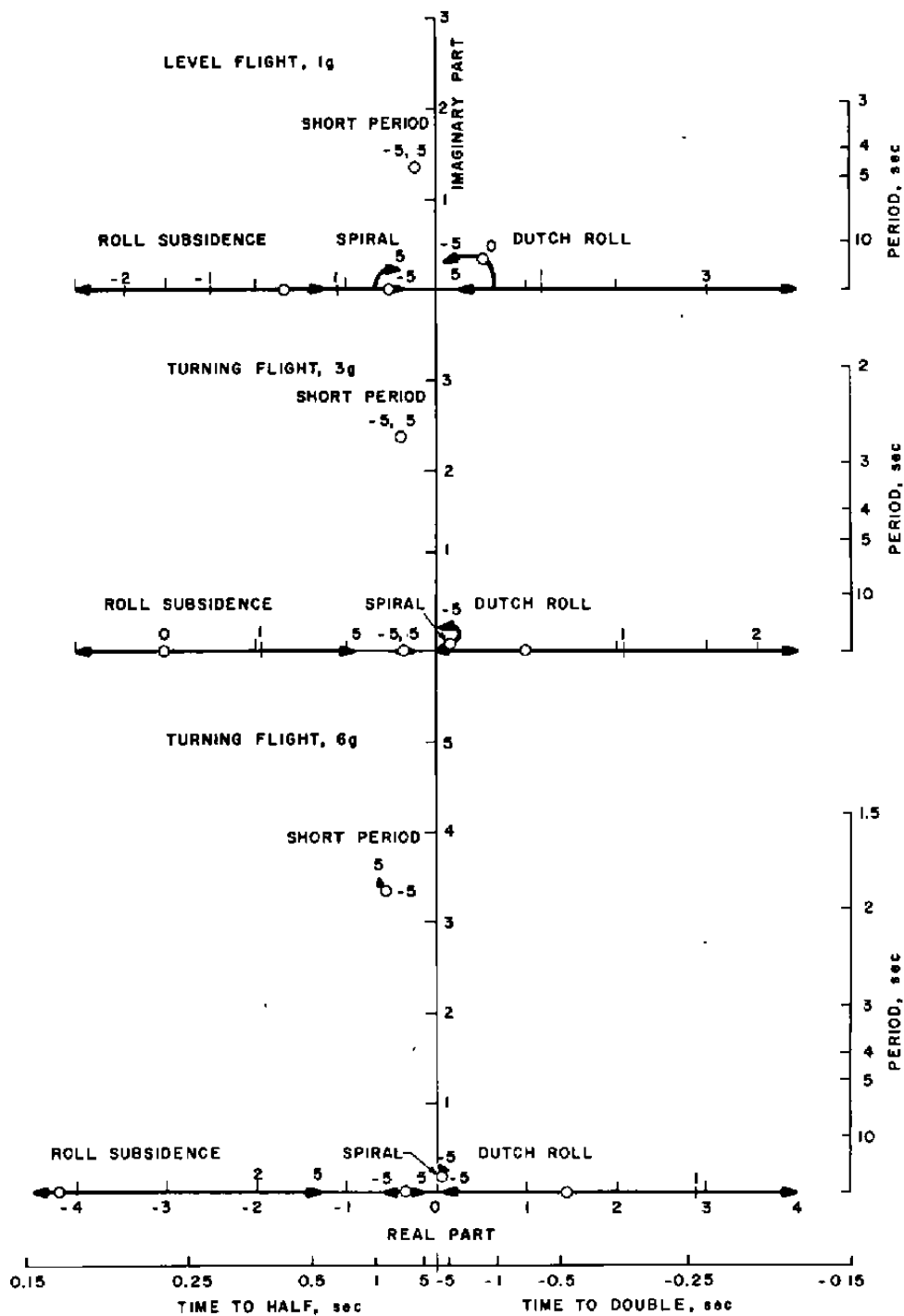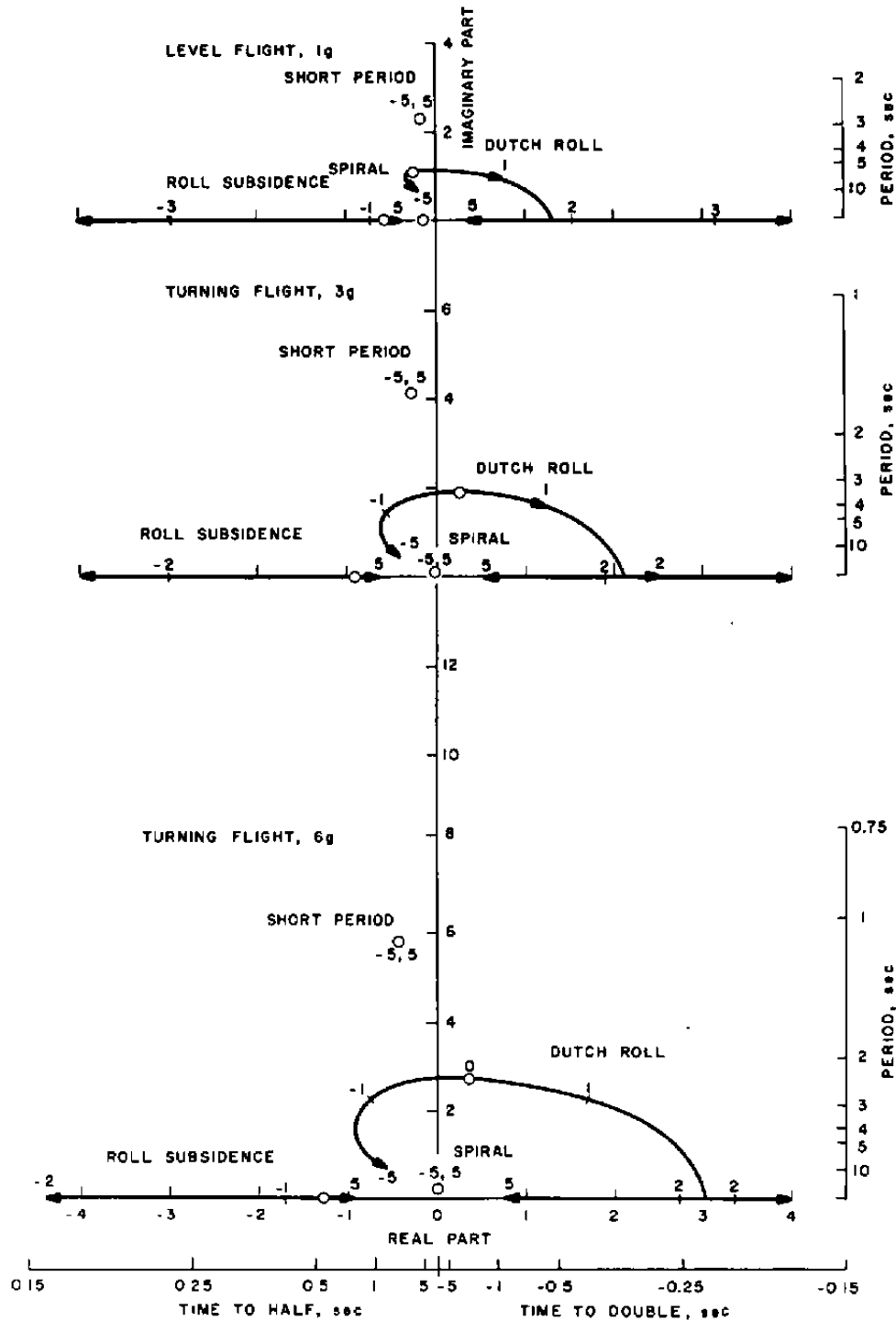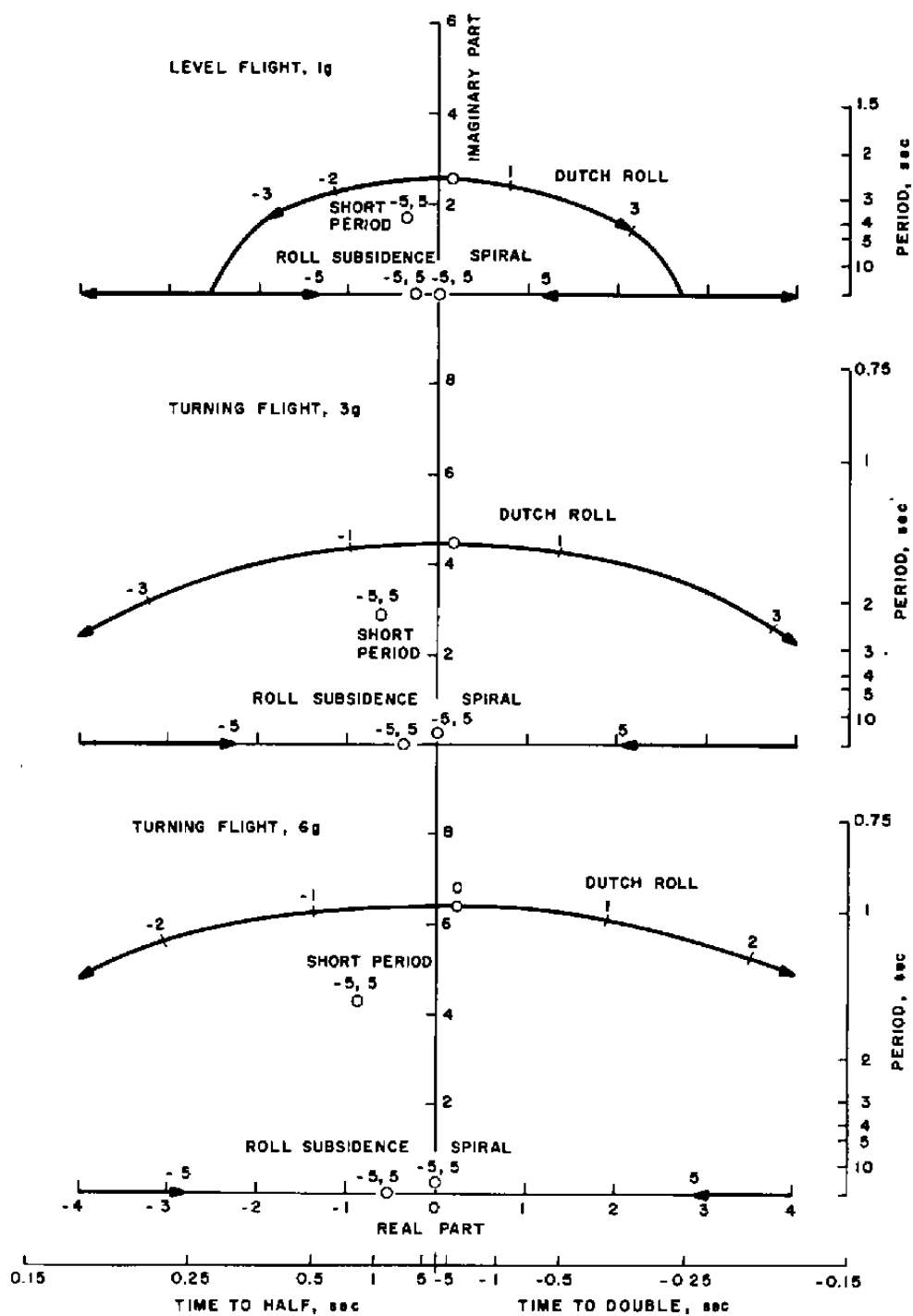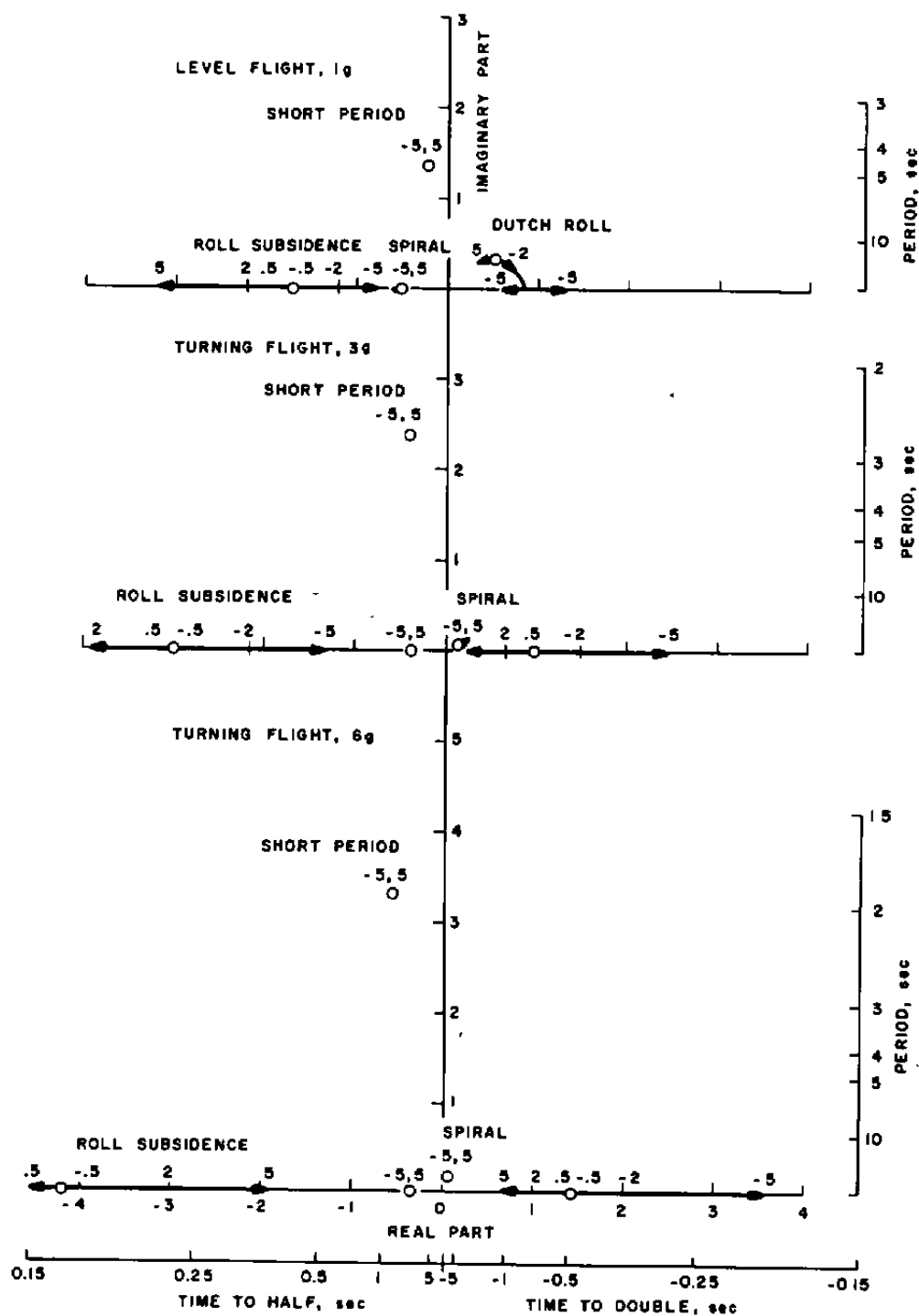
b. A-7
Figure 5. Continued.
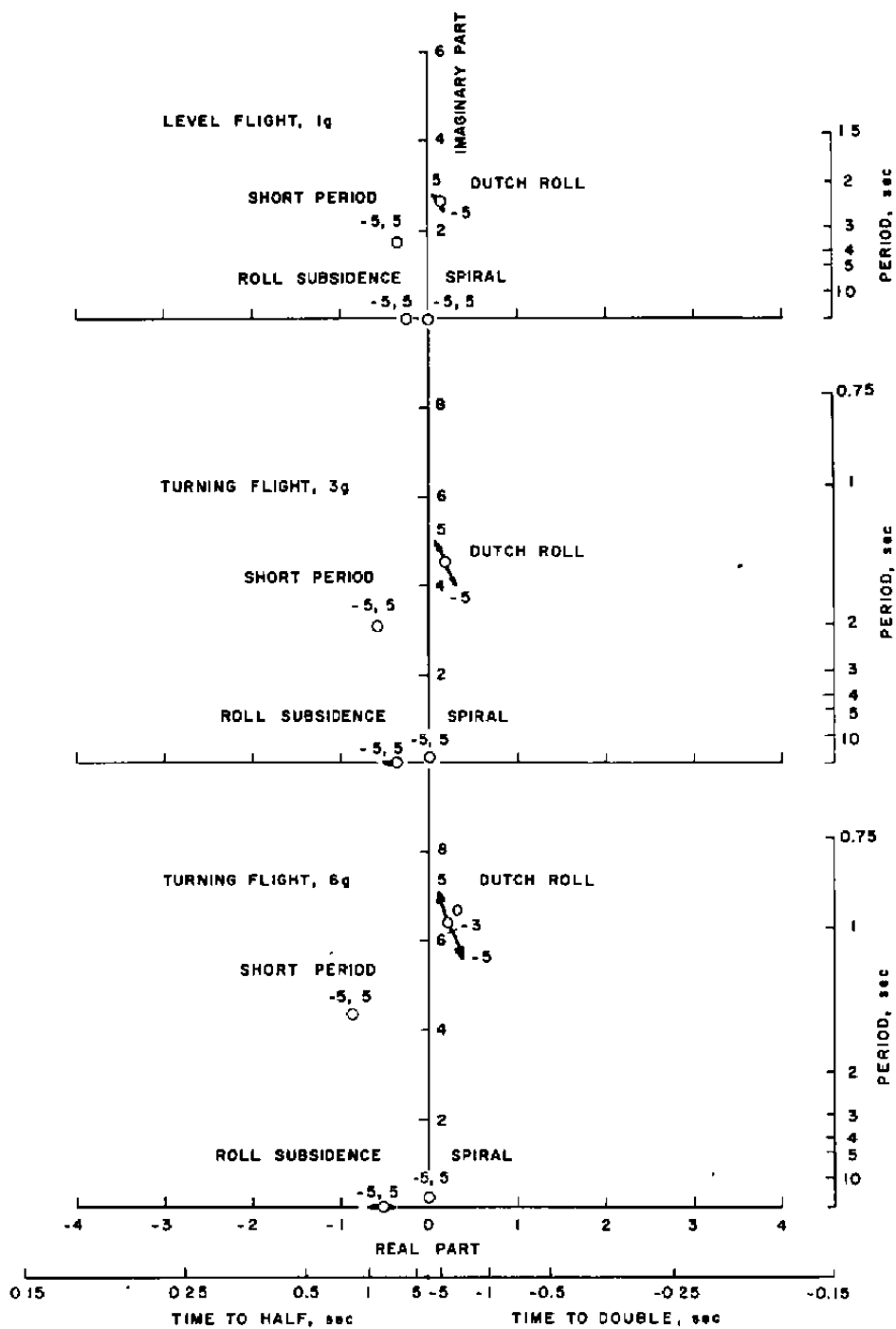
c. F-5

Figure 5. Concluded.
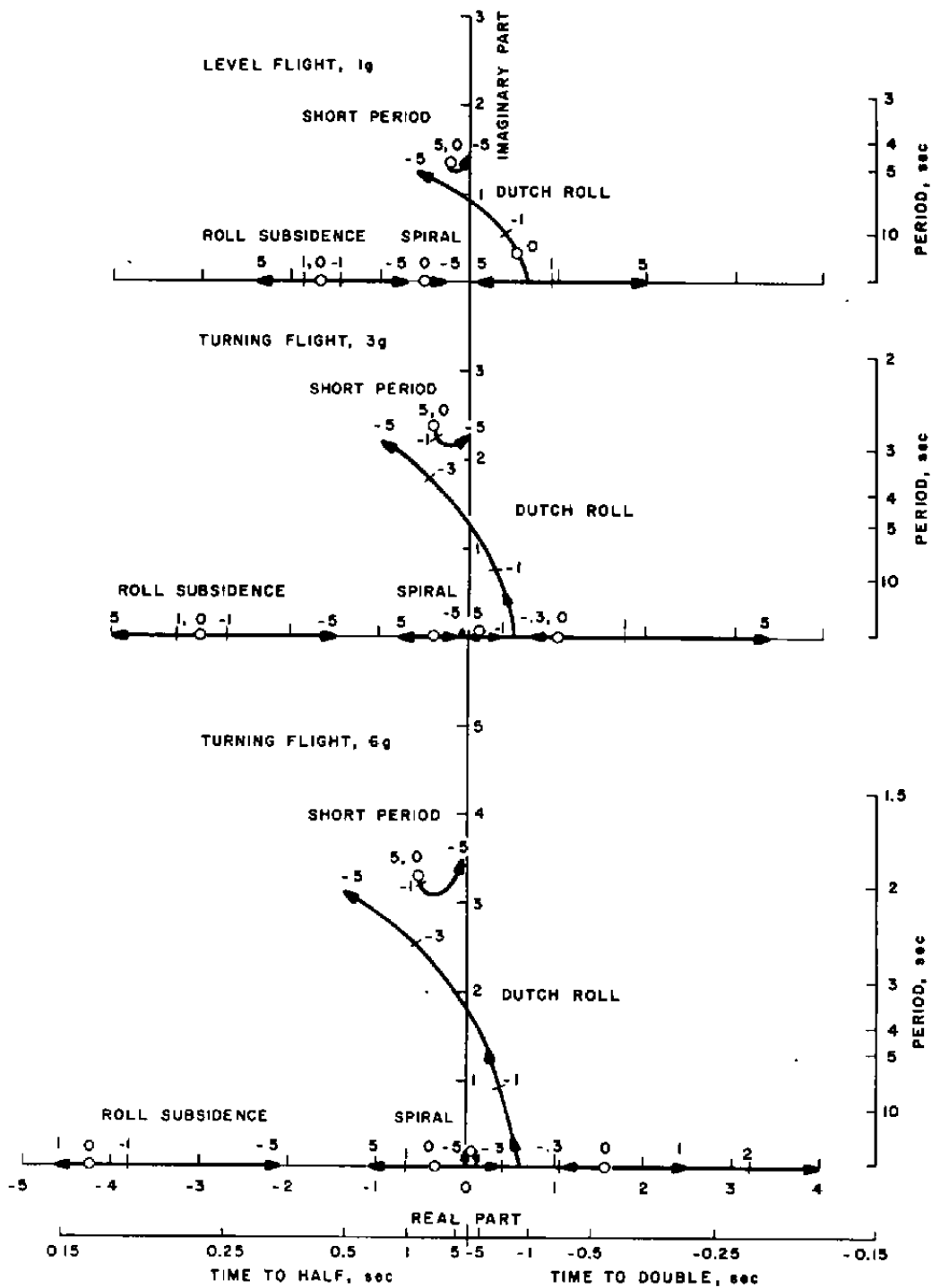
a. F-4

Figure 6. Locus of roots with C_{n_p} variation.

b. A-7
Figure 6. Continued.

c. F-5

Figure 6. Concluded.

a. F-4

Figure 7. Locus of roots with C_{ℓ_β} variation.
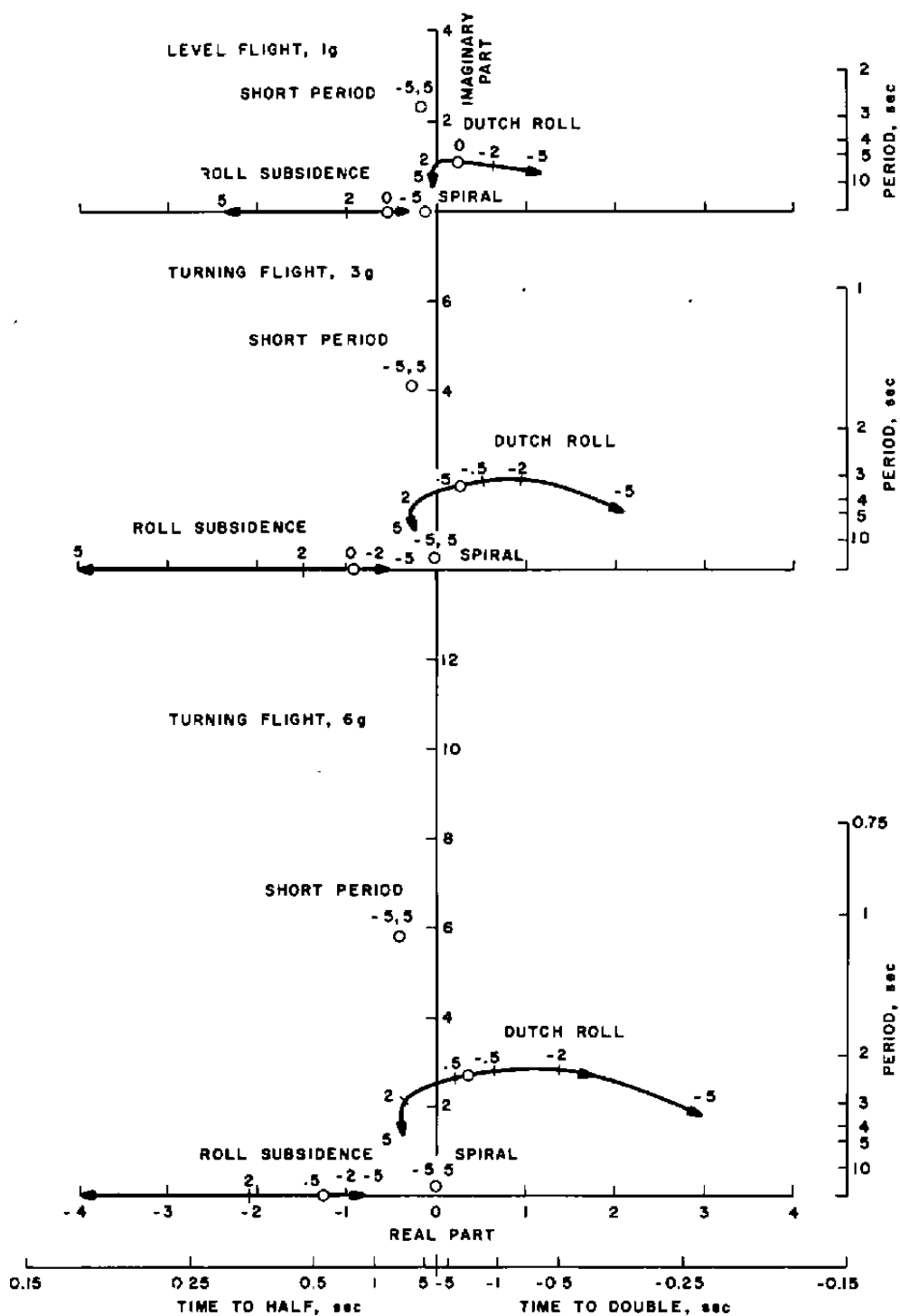
b. A-7
Figure 7. Continued.
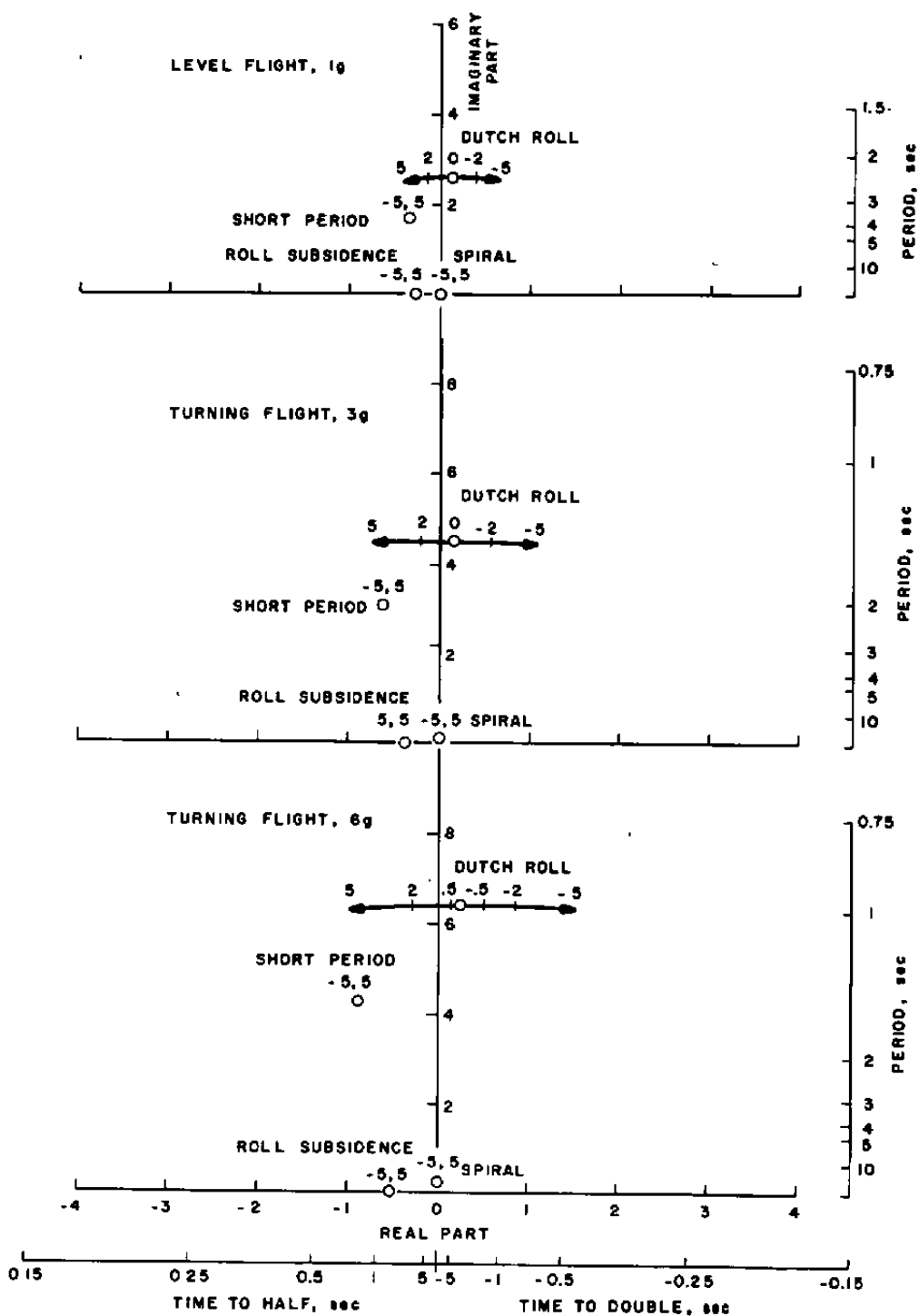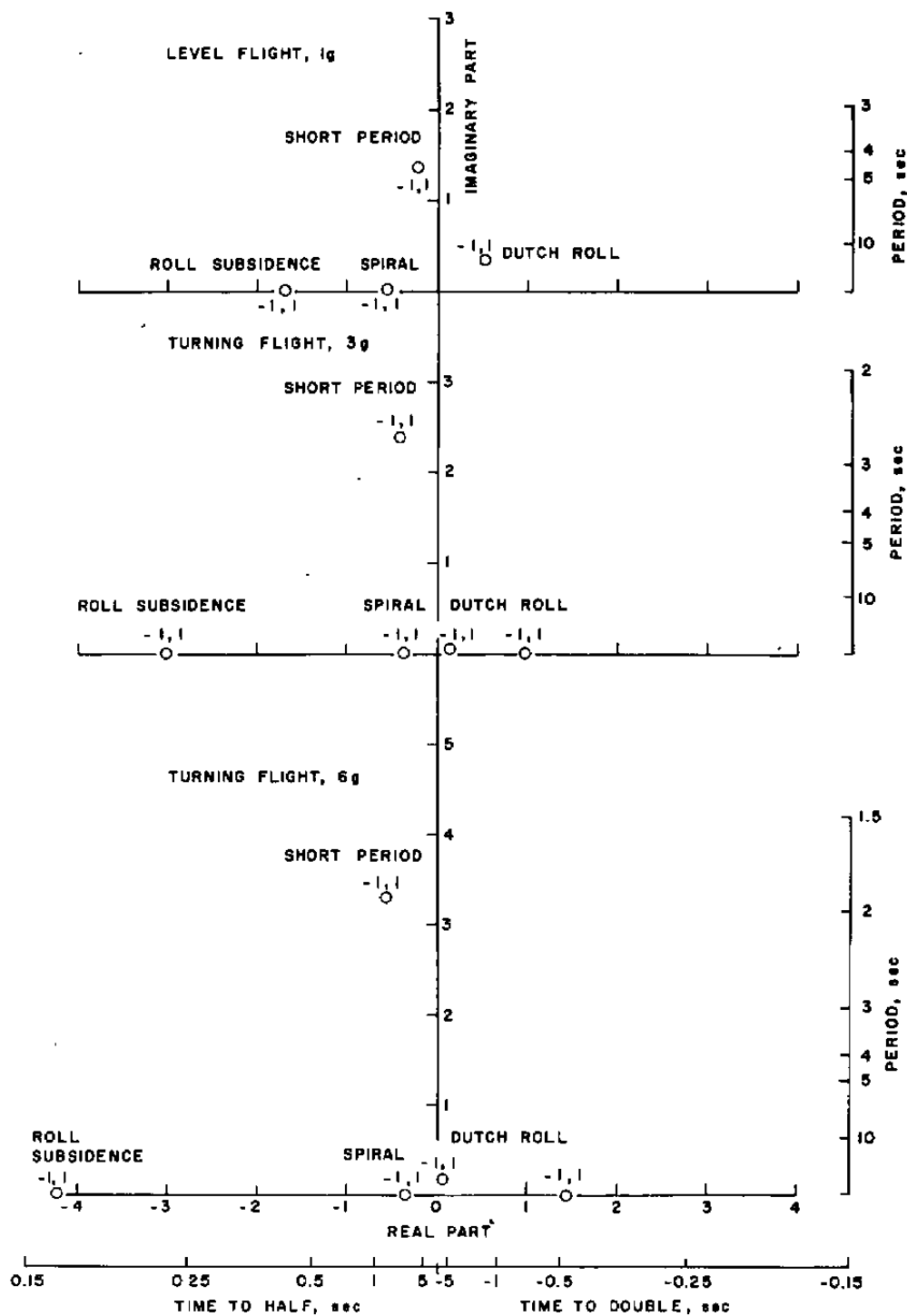
c. F-5

Figure 7. Concluded.

a. F-4

Figure 8. Locus of roots with C_{n_β} variation.

b. A-7
Figure 8. Continued.

c. F-5

Figure 8. Concluded.

a. F-4

Figure 9. Locus of roots with C_{m_p}, C_{m_r}, $C_{\ell_{\dot{\alpha}}}$, and $C_{n_{\dot{\alpha}}}$ variation.
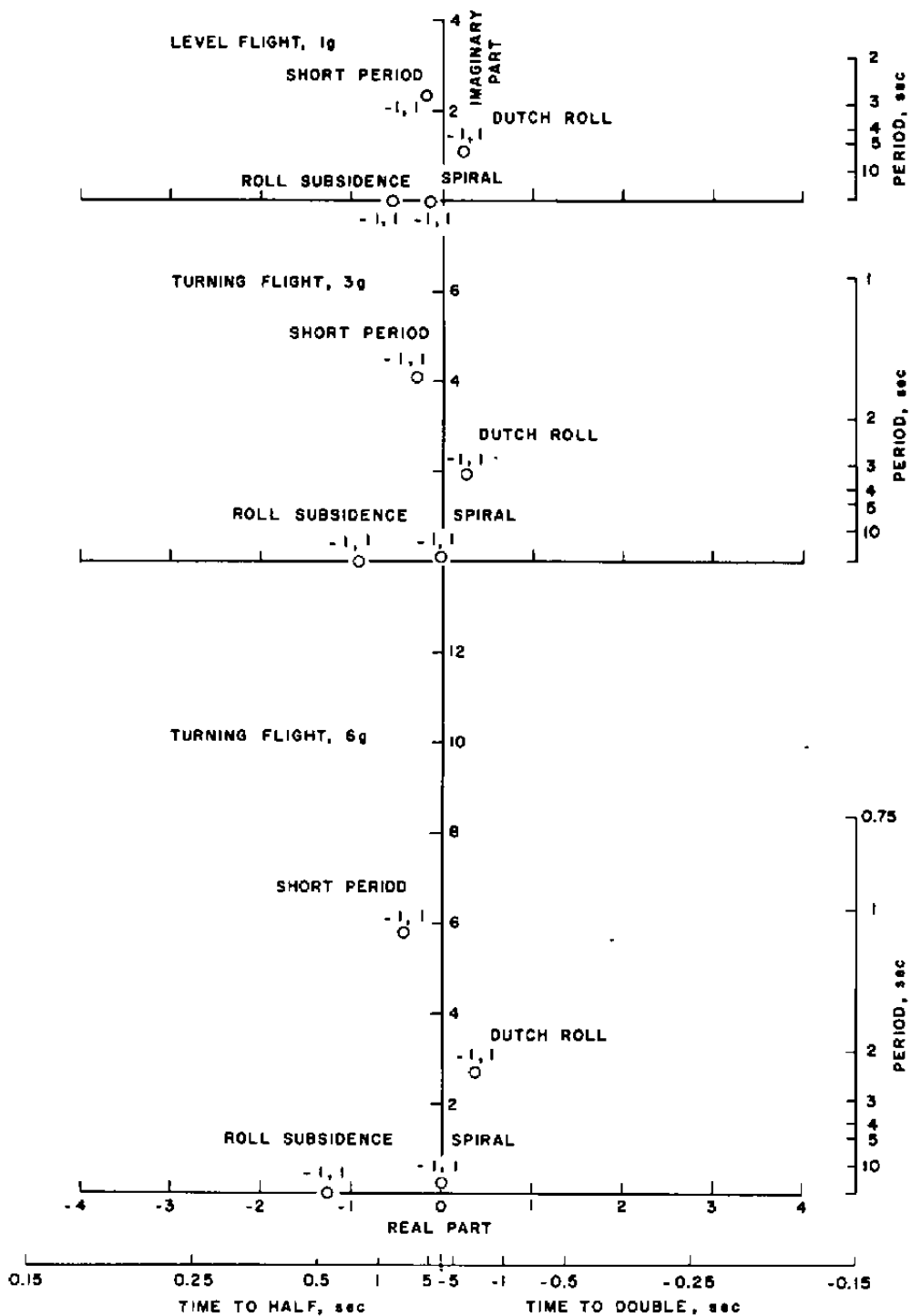
b. A-7
Figure 9. Continued.
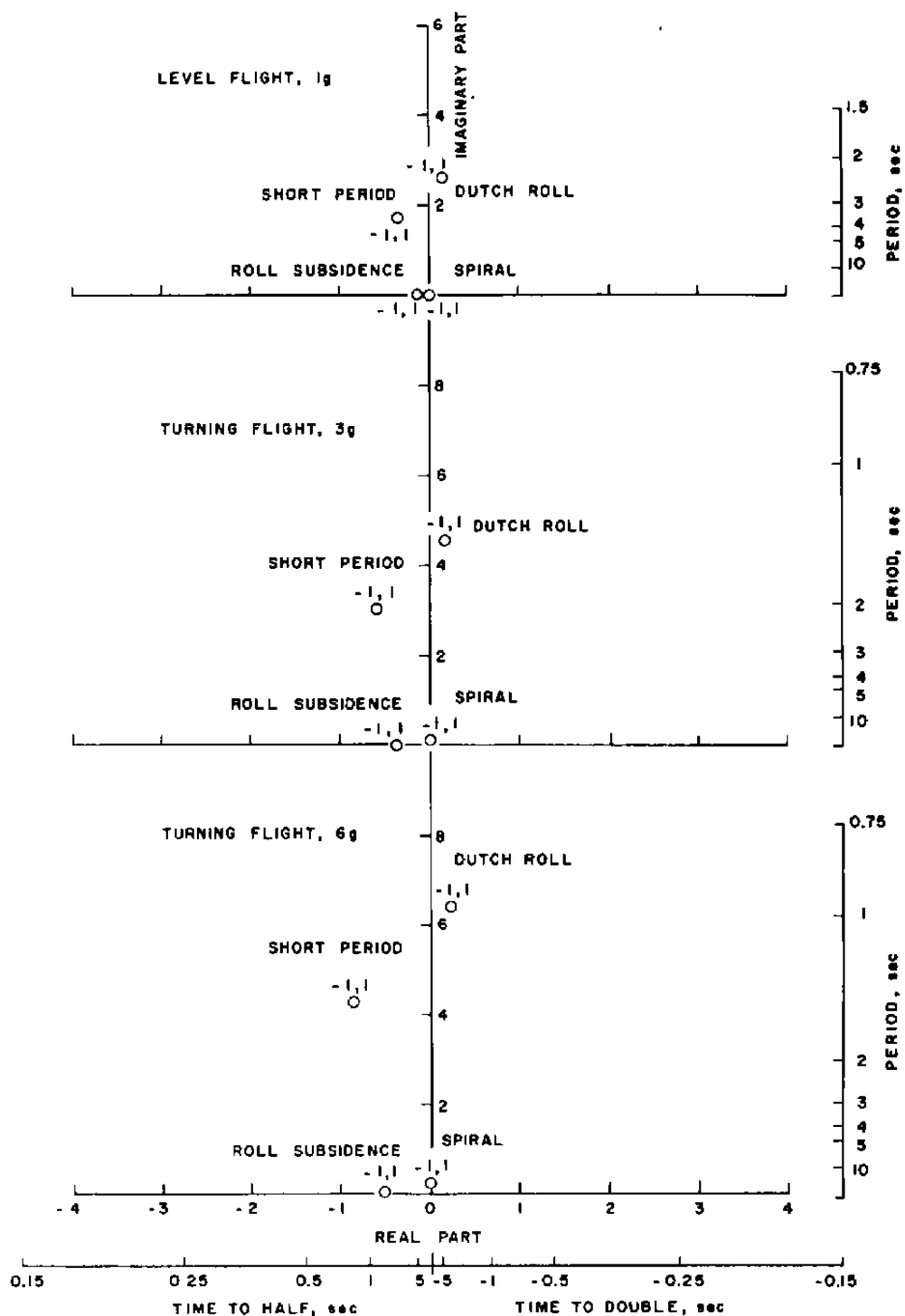
c. F-5

Figure 9. Concluded.
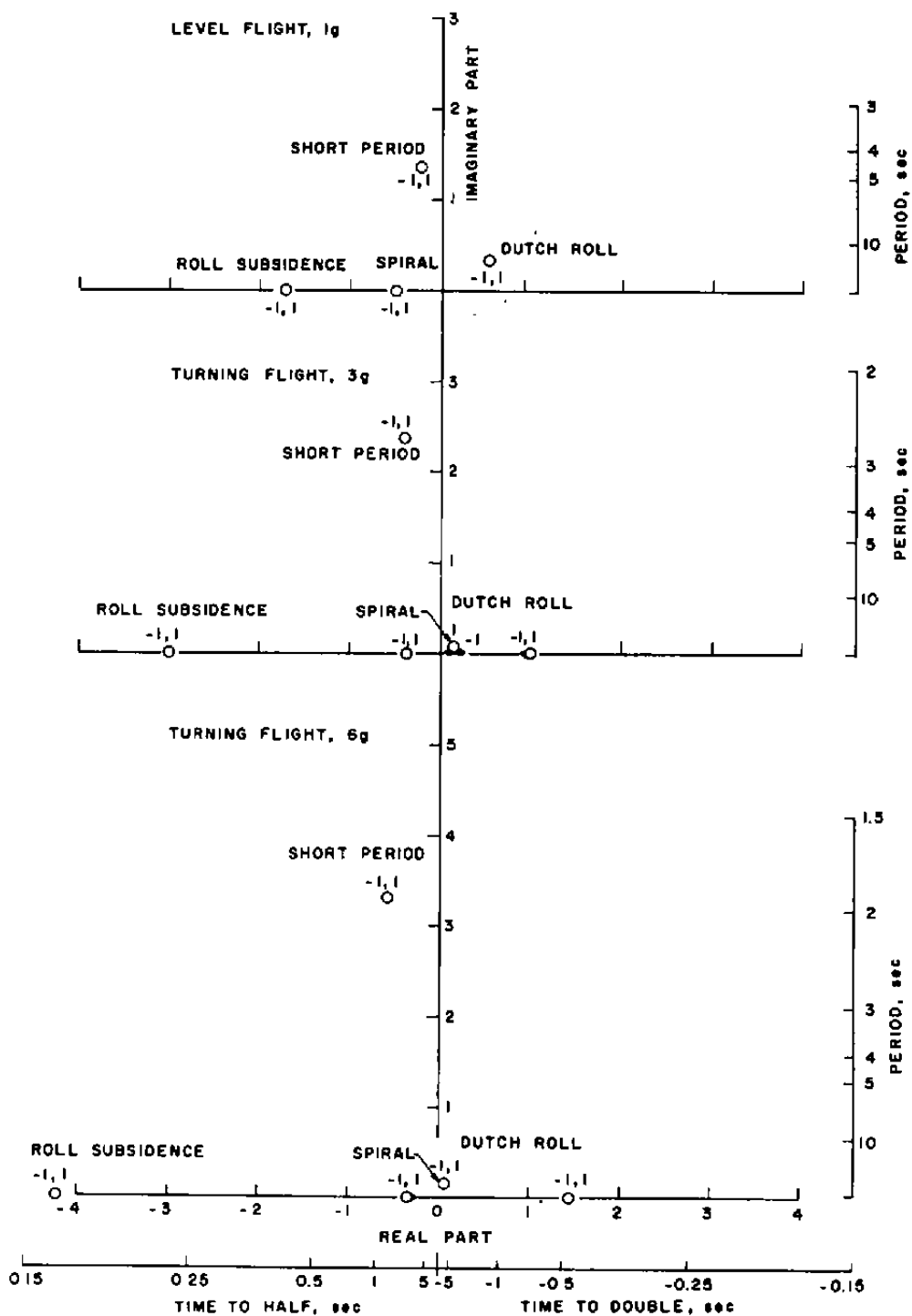
a. F-4

Figure 10. Locus of roots with C_{n_q} variation.

b. A-7

Figure 10. Continued.

c. F-5

Figure 10. Concluded.

a. F-4

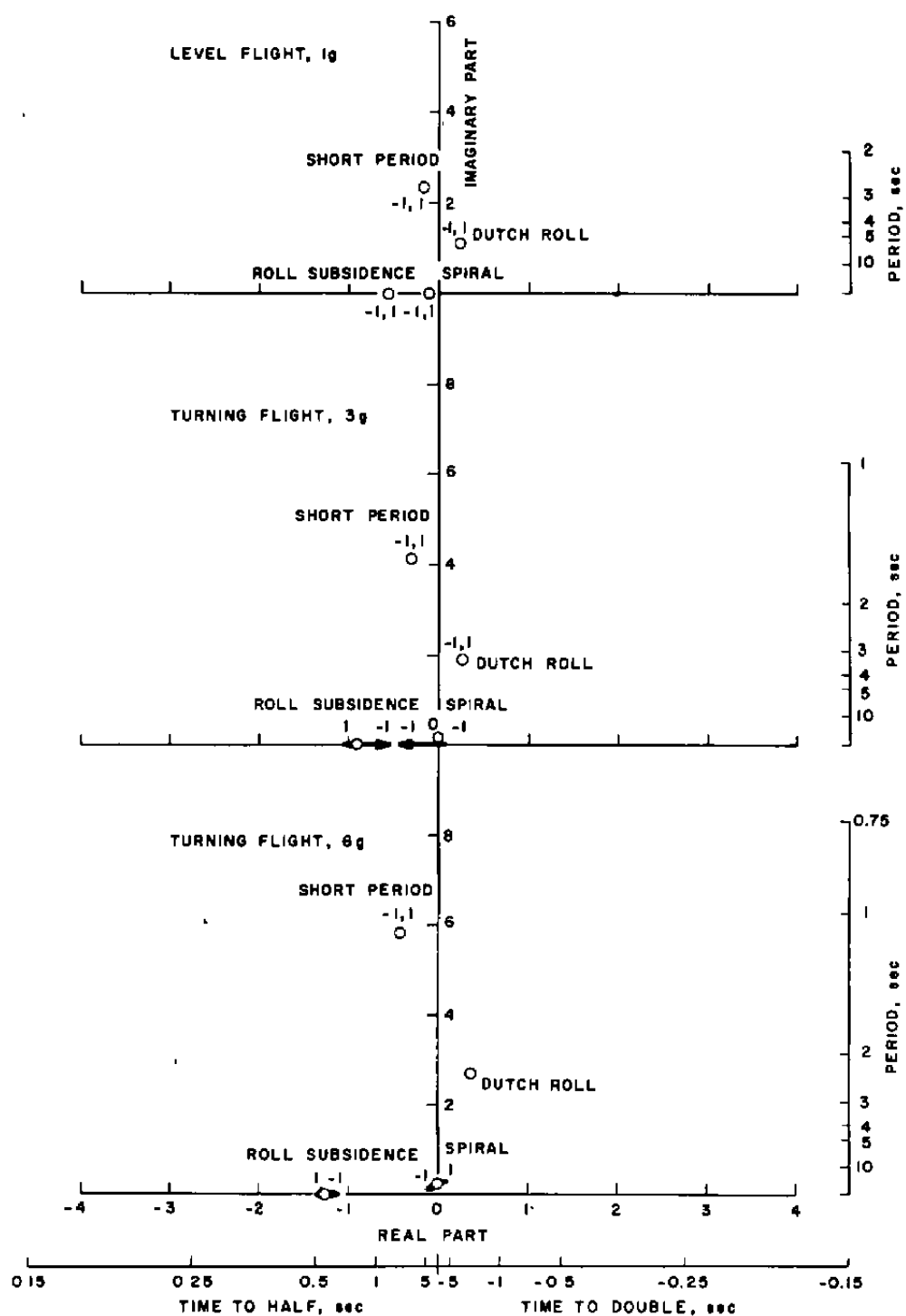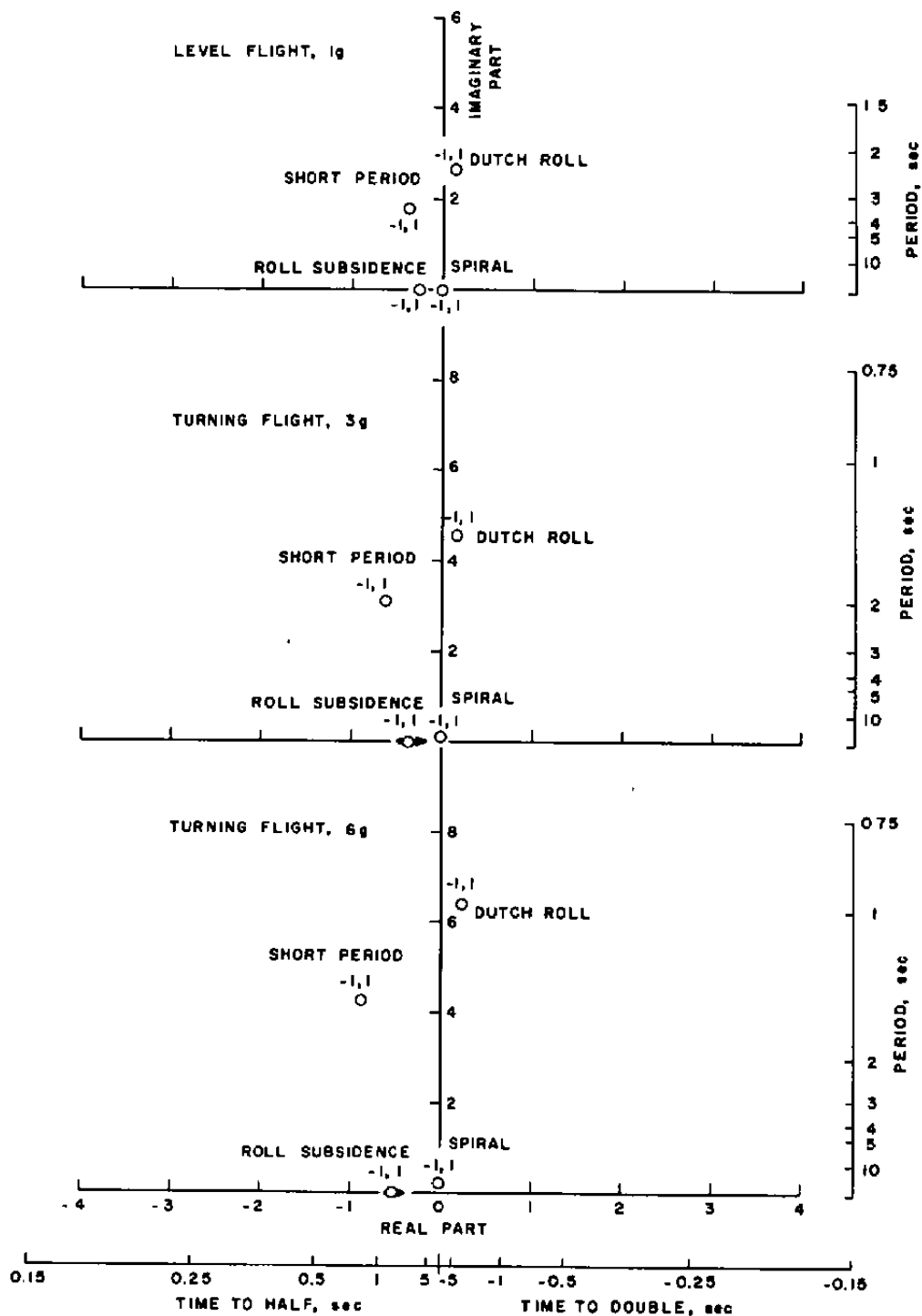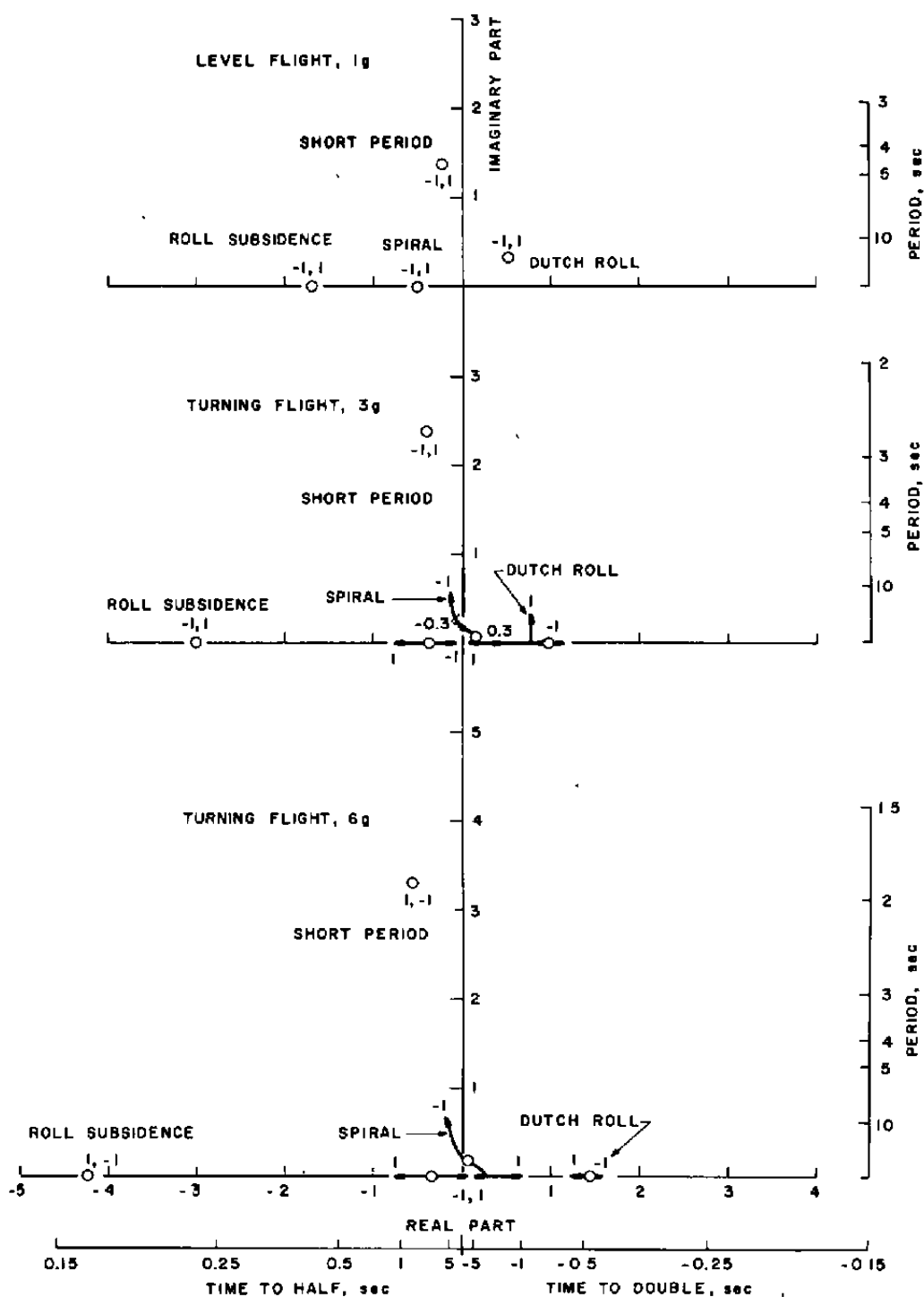Figure 11. Locus of roots with $C\ell_q$ variation.
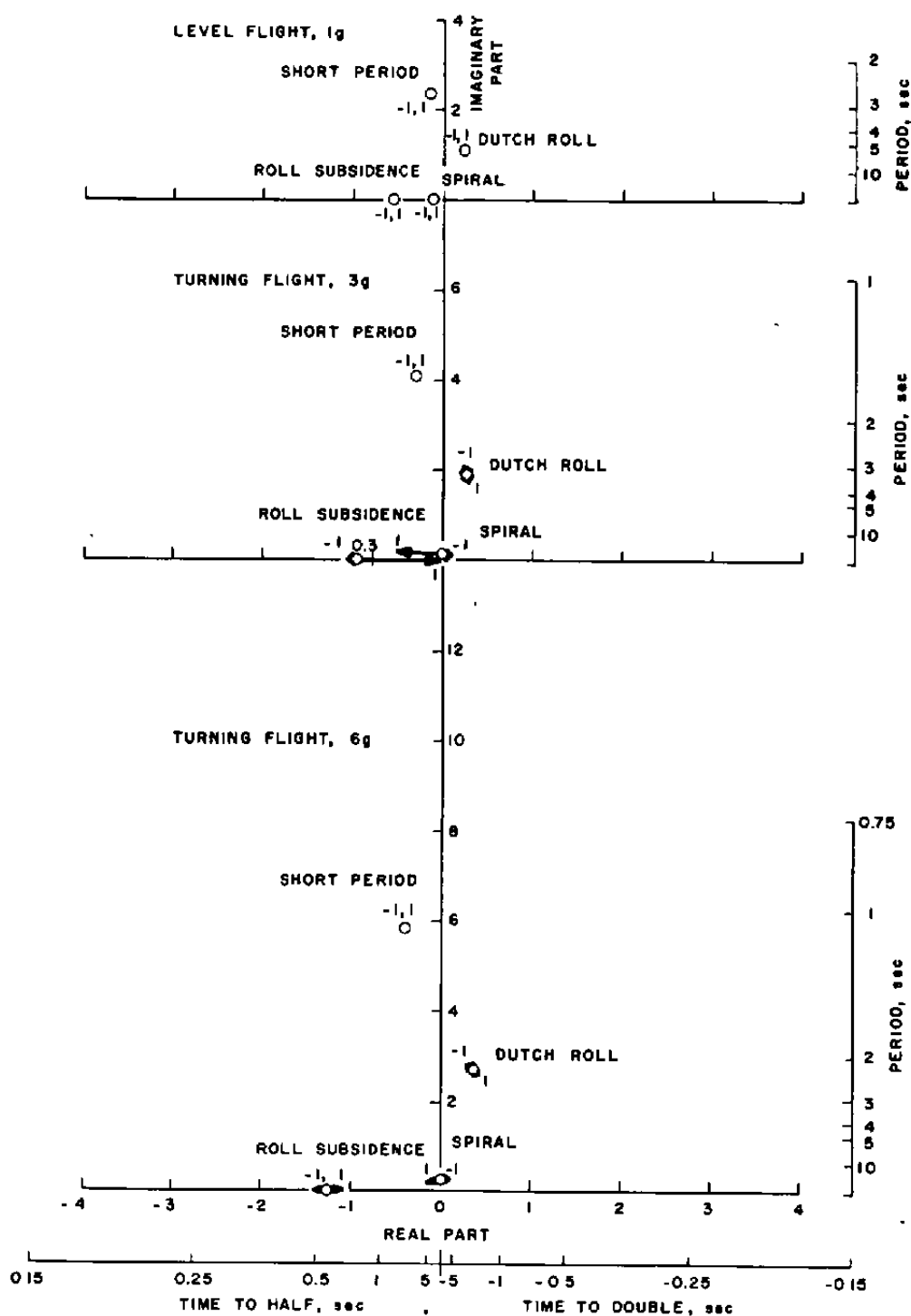
b. A-7
Figure 11. Continued.
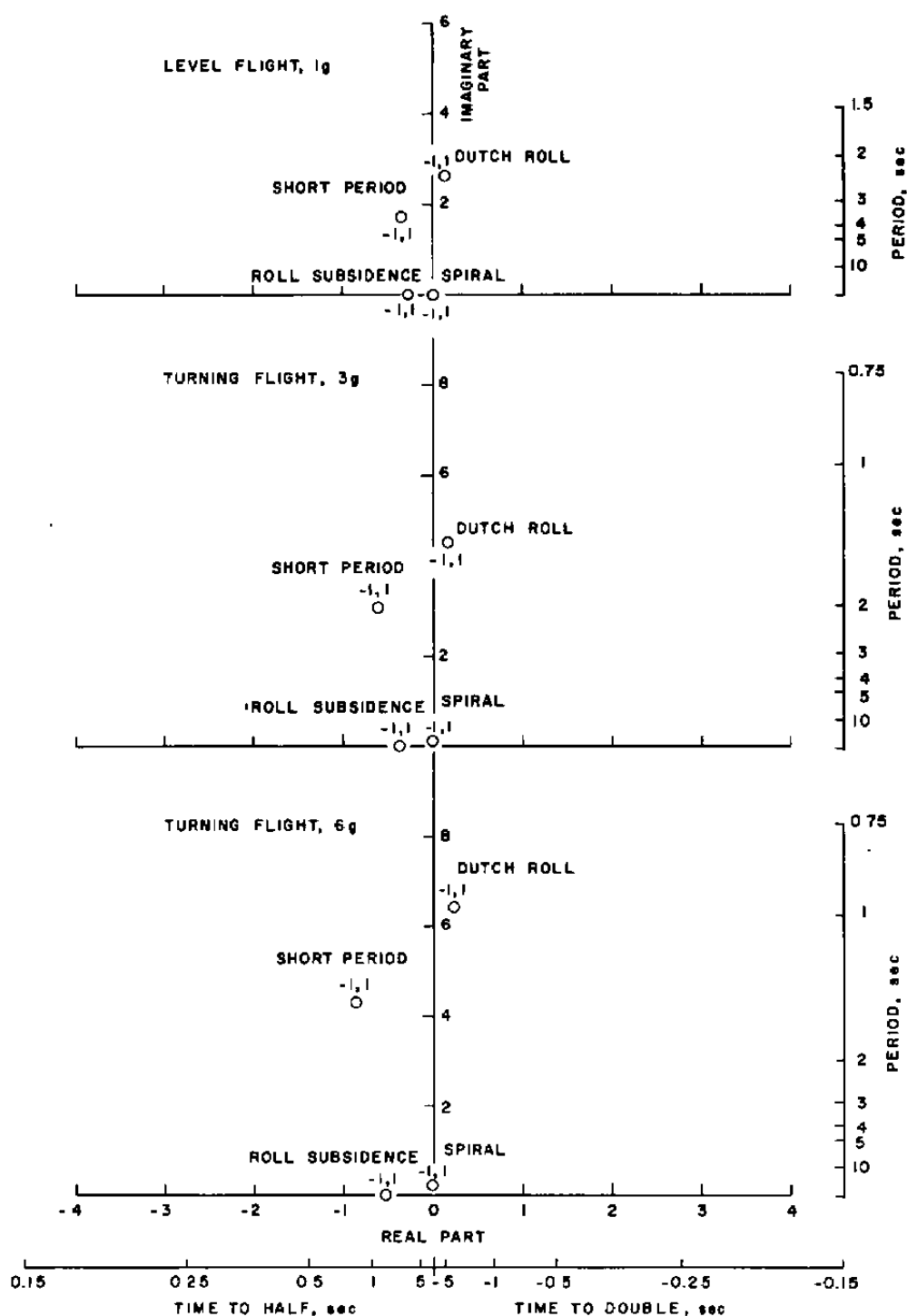
c. F-5

Figure 11. Concluded.

Table 1. F-4 Aircraft Physical and Aerodynamic Characteristics

Weight	$1,215$ slugs	C_{ℓ_r}	0.638
I_x	$29,950$ slug-ft^2	C_{n_β}	-0.252
I_y	$164,300$ slug-ft^2	C_{n_p}	-0.031
I_z	$169,538$ slug-ft^2	C_{n_r}	-0.444
I_{xz}	$5,241$ slug-ft^2	$C_{\ell_{\dot\alpha}}$	0
S	538.34 ft^2	C_{ℓ_q}	0
b	38.41 ft	C_{m_q}	-4.0
$\bar{c}$	16.04 ft	C_{m_α}	-0.5
cg	33 percent MAC	$C_{m_{\dot\alpha}}$	0
α	29 deg	C_{m_r}	0
C_L	0.928	$C_{n_{\dot\beta}}$	0
C_{y_β}	-0.201	C_{N_α}	1.76
C_{y_p}	0.056	C_A	0.05
C_{y_r}	-0.708	$C_{\ell_{\dot\beta}}$	0
C_{ℓ_β}	-0.017	$C_{n_{\dot\alpha}}$	0
C_{ℓ_p}	-0.410	C_{n_q}	0

Table 2. A-7 Aircraft Physical and Aerodynamic Characteristics

Weight	719 slugs	C_{ℓ_r}	0.075
I_x	15,927 slug-ft^2	C_{n_β}	-0.123
I_y	64,792 slug-ft^2	C_{n_p}	0.0175
I_z	75,976 slug-ft^2	C_{n_r}	-0.23
I_{xz}	3,885 slug-ft^2	$C_{\ell_{\dot{\alpha}}}$	0
S	375.00 ft^2	C_{ℓ_q}	0
b	38.73 ft	C_{m_q}	-4.9
$\bar{c}$	10.84 ft	C_{m_α}	-1.56
cg	30 percent MAC	$C_{m_{\dot{\alpha}}}$	0
α	26.5 deg	C_{m_r}	0
C_L	1.07	$C_{n_{\dot{\beta}}}$	0
C_{Y_β}	-0.974	C_{N_α}	0.871
C_{Y_p}	0.14	C_A	-0.04
C_{Y_r}	0.35	$C_{\ell_{\dot{\beta}}}$	0
C_{ℓ_β}	-0.10	$C_{n_{\dot{\alpha}}}$	0
C_{ℓ_p}	-0.01	C_{n_q}	0

Table 3. F-5 Aircraft Physical and Aerodynamic Characteristics

Weight	357 slugs	C_{ℓ_r}	-0.05
I_x	3,400 slug-ft^2	C_{n_β}	0
I_y	37,800 slug-ft^2	C_{n_p}	0.175
I_z	41,000 slug-ft^2	C_{n_r}	0
I_{xz}	-200 slug-ft^2	$C_{\ell_{\dot\alpha}}$	0
S	181.00 ft^2	C_{ℓ_q}	0
b	25.80 ft	C_{m_q}	-18.4
$\bar{c}$	7.88 ft	C_{m_α}	-1.42
cg	18 percent MAC	$C_{m_{\dot\alpha}}$	0
α	28 deg	C_{m_r}	0
C_L	1.08	$C_{n_{\dot\beta}}$	0
C_{Y_β}	-0.29	C_{N_α}	2.98
C_{Y_p}	0.20	C_A	-0.02
C_{Y_r}	1.2	$C_{\ell_{\dot\beta}}$	0
C_{ℓ_β}	-0.18	$C_{n_{\dot\alpha}}$	0
C_{ℓ_p}	0	C_{n_q}	0

44

Table 4. Flight Conditions

	n, g	ϕ, deg	$\overline{q}$, lb/ft^2	V_∞, ft/sec	$\dot{\psi}_o$, rad/sec	q_o, rad/sec	r_o, rad/sec
F-4 AIRCRAFT	1	0	78.3	419.2	0	0	0
	3	70.5	238.8	732.3	0.124	0.117	0.041
	6	80.4	469.6	1,027.9	0.185	0.182	0.031
A-7 AIRCRAFT	1	0	57.6	359.8	0	0	0
	3	70.5	176.4	629.4	0.145	0.137	0.048
	6	80.4	353.0	890.3	0.214	0.211	0.036
F-5 AIRCRAFT	1	0	58.8	363.0	0	0	0
	3	70.5	173.0	623.3	0.146	0.138	0.049
	6	80.4	345.9	881.3	0.216	0.213	0.036

APPENDIX A
5-DOF CHARACTERISTIC DETERMINANT

$$
\begin{vmatrix}
(\lambda - Z_w)\bar{a} & 0 & 0 & \bar{q} & 0 & 0 & e_5\bar{\phi} \\
0 & (\lambda - Y_v)\bar{\beta} & -e_1\bar{p} & 0 & e_3\bar{r} & 0 & -e_2\bar{\phi} \\
-L_{\dot{a}}\alpha & -(\lambda L_{\dot{\beta}} + L_\beta)\bar{\beta} & (\lambda - e_7)\bar{p} & e_8\bar{q} & -(\lambda\frac{I_{xz}}{I_{xx}} - e_9)\bar{r} & 0 & 0 \\
-(\lambda M_{\dot{a}} + M_a)\bar{a} & 0 & e_{10}\bar{p} & (\lambda - M_q)\bar{q} & -e_{11}\bar{r} & 0 & 0 \\
-\lambda N_{\dot{a}}\bar{a} & -(\lambda N_{\dot{\beta}} + N_\beta)\bar{\beta} & -(\lambda\frac{I_{xz}}{I_{zz}} - e_{12})\bar{p} & e_{13}\bar{q} & (\lambda + e_{14})\bar{r} & 0 & 0 \\
0 & 0 & 0 & -\cos\phi_o\bar{q} & \sin\phi_o\bar{r} & \lambda\bar{\theta} & \dot{\psi}_o\bar{\phi} \\
0 & 0 & -\bar{p} & 0 & 0 & -\dot{\psi}_o\bar{\theta} & \lambda\bar{\phi}
\end{vmatrix} = 0
$$

Coefficients of Characteristic Equation [Eq. (11)]

$$AB1 = -e_5 b_{11} + e_2 b_{31}$$

$$AB2 = e_5 Y_v b_{11} - e_5(b_{12} - e_3 b_{21}) - e_2(b_{31}Z_w + b_{32} - b_{41})$$

$$AB3 = e_5(Y_v b_{12} - b_{13} - e_3 b_{22}) - e_2(Z_w b_{32} - b_{33} + b_{42})$$

$$AB4 = e_5(b_{13}Y_v - b_{14} - e_3 b_{23}) - e_2(Z_w b_{33} - b_{34} + b_{43})$$

$$AB5 = e_5(Y_v b_{14} - e_3 b_{24}) - e_2(b_{34}Z_w + b_{44})$$

$$AC1 = -C_{11}(Y_v + Z_w) + C_{12} + C_{21}e_1 - C_{31}e_3 - C_{41}$$

$$AC2 = C_{11}Z_w Y_v - C_{12}(Y_v + Z_w) + C_{13} + e_1(C_{22} - C_{21}Z_w - C_{51}) \\ + e_3(C_{31}Z_w = C_{32} - C_{61}) + C_{41}Y_v - C_{42}$$

$$AC3 = C_{12}Z_w Y_v - C_{13}(Y_v + Z_w) + C_{14} + e_1(C_{23} - C_{22}Z_w - C_{52}) \\ + e_3(C_{32}Z_w - C_{33} - C_{62}) + C_{42}Y_v - C_{43}$$

$$AC4 = C_{13}Z_w Y_v - C_{14}(Y_v - Z_w) + e_1(C_{24} - C_{23}Z_w - C_{53}) \\ + e_3(C_{33}Z_w - C_{34} - C_{63}) + C_{43}Y_v - C_{44}$$

$$AC5 = C_{14}Z_w Y_v - e_1(C_{24}Z_w - C_{54}) + e_3(C_{34}Z_w - C_{64}) + C_{44}Y_v$$

$$AD1 = (DBB1) \cos \phi_o e_5$$

$$AD2 = DBA1 + e_5[(DBB2) \cos \phi_o - (DBB1) Y_v \cos \phi_o] + DBC1 + DBD1$$

$$AD3 = DBA2 - e_5[(DBB3) \cos \phi_o - (DBB2) Y_v \cos \phi_o] + DBC2 + DBD2$$

$$AD4 = DBA3 + e_5[(DBB4) \cos \phi_o - (DBB3) Y_v \cos \phi_o] + DBC3 + DBD3$$

$$AD5 = DBA4 - e_5(DBB4) Y_v \cos \phi_o + DBC4 + DBD4$$

$$AE1 = \sin \phi_o \, e_2(DBF1) + \sin \phi_o \, e_5(DBH1)$$

$$AE2 = e_2[\sin \phi_o(DBF2) + Z_w \sin \phi_o (DBF1)] - DBG1$$
$$- e_5[\sin \phi_o (DBH2) - Y_v \sin \phi_o (DBH1)] - DBI1$$

$$AE3 = e_2[\sin \phi_o (DBF3) + Z_w \sin \phi_o (DBF2)] + DBG2$$
$$+ e_5[\sin \phi_o (DBH3) - Y_v \sin \phi_o (DBH2)] + DBI2$$

$$AE4 = e_2[\sin \phi_o (DBF4) - Z_w \sin \phi_o (DBF3)] + DBG3$$
$$- e_5[\sin \phi_o (DBH4) + Y_v \sin \phi_o (DBH3)] + DBI3$$

$$AE5 = -Z_w e_2 \sin \phi_o \, DBF4 + DBG4 + Y_v e_5 \sin \phi_o \, DBH4 + DBI4$$

$$b_{11} = -L_{\dot\alpha} - N_{\dot\alpha} (I_{xz}/I_{xx})$$

$$b_{12} = -L_{\dot\alpha} e_{14} + M_q L_{\dot\alpha} + (I_{xz}/I_{xx}) M_{\dot\alpha} e_{13} + e_9 N_{\dot\alpha} + N_\alpha M_q (I_{xz}/I_{xx}) + M_{\dot\alpha} e_8$$

$$b_{13} = M_q e_{14} L_{\dot\alpha} - e_8 e_{11} N_{\dot\alpha} + (I_{xz}/I_{xx}) M_\alpha e_{13} - e_9 e_{13} M_{\dot\alpha} - e_9 M_q N_{\dot\alpha}$$
$$+ e_{11} e_{13} L_{\dot\alpha} + e_8 M_\alpha + e_8 e_{14} M_{\dot\alpha}$$

$$b_{14} = e_8 e_{14} M_\alpha - e_9 e_{13} M_\alpha$$

$$b_{21} = L_{\dot\beta} N_{\dot\alpha} - L_{\dot\alpha} N_{\dot\beta}$$

$$b_{22} = L_{\dot\beta} M_q N_{\dot\alpha} + L_\beta N_{\dot\alpha} + M_{\dot\alpha} N_{\dot\beta} e_8 + M_q N_{\dot\beta} L_{\dot\alpha} - N_\beta L_{\dot\alpha} - M_{\dot\alpha} L_{\dot\beta} e_{13}$$

$$b_{23} = -L_\beta M_q N_{\dot\alpha} + e_8 M_{\dot\alpha} N_\beta + e_8 M_\alpha N_{\dot\beta} + L_{\dot\alpha} N_\beta M_q - L_\beta M_{\dot\alpha} e_{13} - L_{\dot\beta} M_\alpha e_{13}$$

$$b_{24} = e_8 M_\alpha N_\beta - e_{13} M_\alpha L_\beta$$

$$b_{31} = -L_{\dot\beta} - N_{\dot\beta}(I_{xz}/I_{xx})$$

$$b_{32} = L_{\dot\beta} M_q - L_\beta - L_{\dot\beta} e_{14} - (I_{xz}/I_{xx}) N_\beta + (I_{xz}/I_{xx}) N_{\dot\beta} M_q + e_9 N_{\dot\beta}$$

$$b_{33} = L_\beta M_q + e_{14} L_{\dot\beta} M_q - e_{14} L_\beta + e_8 e_{11} N_{\dot\beta} - N_{\dot\beta} M_q e_9 + N_\beta e_9$$
$$+ (I_{xz}/I_{xx}) N_\beta M_q - e_{11} e_{13} L_{\dot\beta}$$

$$b_{34} = e_{14}L_\beta M_q + e_8 e_{11} N_\beta - e_9 N_\beta M_q - e_{11} e_{13} L_\beta$$

$$b_{41} = -N_{\dot\beta} M_{\dot\alpha}(I_{xz}/I_{xx}) - M_{\dot\alpha} L_{\dot\beta}$$

$$b_{42} = -L_{\dot\beta} e_{11} N_{\dot\alpha} - N_{\dot\beta} e_9 M_\alpha - (I_{xz}/I_{xx}) M_{\dot\alpha} N_\beta + e_9 M_{\dot\alpha} N_\beta + L_{\dot\alpha} N_\beta e_{11}$$

$$b_{43} = -L_\beta e_{11} N_{\dot\alpha} + N_{\dot\beta} e_9 M_\alpha - (I_{xz}/I_{xx}) M_\alpha N_\beta + e_9 M_{\dot\alpha} N_\beta + L_{\dot\alpha} N_\beta e_{11}$$
$$- e_{14} M_\alpha L_{\dot\beta} - L_\beta M_\alpha - L_\beta e_{14} M_{\dot\alpha}$$

$$b_{44} = e_9 M_\alpha N_\beta - L_\beta e_{14} M_\alpha$$

$$C_{11} = 1 - [(I_{xz} I_{xz})/(I_{xx} I_{zz})]$$

$$C_{12} = e_{14} - M_q - e_7 + (I_{xz}/I_{zz}) e_9 + [(I_{xz} I_{xz})/(I_{xx} I_{zz})]$$

$$C_{13} = e_7 M_q - e_{14} M_q - e_7 e_{14} + e_8 e_{11}(I_{xz}/I_{zz}) - e_{10} e_{13}(I_{xz}/I_{xx})$$
$$- (I_{xz}/I_{xx}) M_q e_{12} - e_9 M_q (I_{xz}/I_{zz}) - e_9 e_{12} + e_{11} e_{13} - e_8 e_{10}$$

$$C_{14} = e_7 e_{14} M_q - e_8 e_{11} e_{12} + e_9 e_{10} e_{13} + e_9 e_{12} M_q - e_7 e_{11} e_{13} - e_8 e_{10} e_{14}$$

$$C_{21} = -L_{\dot\beta} - N_{\dot\beta}(I_{xz}/I_{xx})$$

$$C_{22} = L_{\dot\beta} M_q - L_\beta - L_{\dot\beta} e_{14} - (I_{xz}/I_{xx}) N_\beta + (I_{xz}/I_{xx}) N_{\dot\beta} M_q + e_9 N_{\dot\beta}$$

$$C_{23} = L_\beta M_q + e_{14} L_{\dot\beta} M_q - e_{14} L_\beta + e_8 e_{11} N_{\dot\beta} - N_{\dot\beta} M_q e_9 + N_\beta e_9$$
$$+ (I_{xz}/I_{xx}) N_\beta M_q - e_{11} e_{13} L_{\dot\beta}$$

$$C_{24} = e_{14} L_\beta M_q + e_8 e_{11} N_\beta - e_9 N_\beta M_q - e_{11} e_{13} L_\beta$$

$$C_{31} = -N_{\dot\beta} - (I_{xz}/I_{zz}) L_{\dot\beta}$$

$$C_{32} = N_{\dot\beta} M_q + N_{\dot\beta} e_7 - N_\beta - (I_{xz}/I_{zz}) L_\beta + (I_{xz}/I_{zz}) M_q L_{\dot\beta} + e_{12} L_{\dot\beta}$$

$$C_{33} = -e_{10} e_{13} L_{\dot\beta} + N_\beta M_q + N_\beta e_7 - e_7 M_q N_{\dot\beta} + e_8 e_{10} N_{\dot\beta}$$
$$- e_{12} M_q L_{\dot\beta} + L_\beta e_{12} + (I_{xz}/I_{zz}) M_q L_\beta$$

$$C_{34} = -e_{10} e_{13} L_\beta + e_8 e_{10} N_\beta - L_\beta e_{12} M_q$$

$$C_{41} = DBB1 = M_{\dot\alpha} C_{11}$$

$$C_{42} = DBB2 = -L_{\dot\alpha} e_{10} + e_{11} N_{\dot\alpha} - M_\alpha[(I_{xz} I_{xz})/(I_{xx} I_{zz})] + e_9 M_{\dot\alpha}(I_{xz}/I_{zz}) + e_{12} M_{\dot\alpha}(I_{xz}/I_{xx})$$
$$-N_{\dot\alpha} e_{10}(I_{xz}/I_{xx}) + e_{11} L_{\dot\alpha}(I_{xz}/I_{zz}) + M_\alpha + e_{14} M_{\dot\alpha} - e_7 M_{\dot\alpha}$$

$$C_{43} = DBB3 = -L_{\dot{\alpha}} e_{14} e_{10} - e_7 e_{11} N_{\dot{\alpha}} + e_9 M_\alpha (I_{xz}/I_{zz}) + e_{12} M_\alpha (I_{xz}/I_{xx}) - e_9 e_{12} M_{\dot{\alpha}}$$
$$+ e_9 e_{10} N_{\dot{\alpha}} - e_{11} e_{12} L_{\dot{\alpha}} - e_7 M_\alpha - e_7 e_{14} M_{\dot{\alpha}} + M_\alpha e_{14}$$

$$C_{44} = DBB4 = -e_9 e_{12} M_{\dot{\alpha}} - e_7 e_{14} M_{\dot{\alpha}}$$

$$C_{51} = -N_{\dot{\beta}} M_{\dot{\alpha}} (I_{xz}/I_{xx}) - M_{\dot{\alpha}} L_{\dot{\beta}}$$

$$C_{52} = -L_{\dot{\beta}} e_{11} N_{\dot{\alpha}} - (I_{xz}/I_{xx}) M_\alpha N_{\dot{\beta}} + e_9 M_{\dot{\alpha}} N_{\dot{\beta}} - N_{\dot{\beta}} M_{\dot{\alpha}} (I_{xz}/I_{xx}) + L_{\dot{\alpha}} N_{\dot{\beta}} e_{11}$$
$$- L_{\dot{\beta}} M_\alpha - e_{14} M_{\dot{\alpha}} L_{\dot{\beta}} - L_\beta M_{\dot{\alpha}}$$

$$C_{53} = -L_\beta e_{11} N_\alpha + N_{\dot{\beta}} e_9 M_\alpha - (I_{xz}/I_{xx}) M_\alpha N_\beta + e_9 M_{\dot{\alpha}} N_\beta + L_{\dot{\alpha}} N_\beta e_{11} - e_{14} M_\alpha L_{\dot{\beta}}$$
$$- L_\beta M_\alpha - L_\beta e_{14} M_{\dot{\alpha}}$$

$$C_{54} = e_9 M_\alpha N_\beta - L_\beta e_{14} M_\alpha$$

$$C_{61} = M_{\dot{\alpha}} N_{\dot{\beta}} + M_{\dot{\alpha}} L_{\dot{\beta}} (I_{xz}/I_{zz})$$

$$C_{62} = L_{\dot{\beta}} N_{\dot{\alpha}} e_{10} + N_{\dot{\beta}} M_\alpha + e_7 M_{\dot{\alpha}} N_{\dot{\beta}} + M_\alpha N_\beta - N_{\dot{\beta}} L_{\dot{\alpha}} e_{10}$$
$$+ L_{\dot{\beta}} M_\alpha (I_{xz}/I_{zz}) - L_{\dot{\beta}} e_{12} M_{\dot{\alpha}} + L_\beta M_{\dot{\alpha}} (I_{xz}/I_{zz})$$

$$C_{63} = L_\beta e_{10} N_{\dot{\alpha}} - e_7 M_\alpha N_{\dot{\beta}} + M_\alpha N_\beta + e_7 M_{\dot{\alpha}} N_\beta - L_{\dot{\alpha}} N_\beta e_{10} - e_{17} M_\alpha L_{\dot{\beta}}$$
$$+ L_\beta M_\alpha (I_{xz}/I_{zz}) - e_{12} M_{\dot{\alpha}} L_\beta$$

$$C_{64} = -e_{12} M_\alpha L_\beta - e_7 M_{\dot{\alpha}} N_\beta$$

$$DBA1 = -Tempa (e_2 \cos \phi_o)$$

$$DBA2 = e_2 \cos \phi_o [Tempa \; Z_w - Tempb]$$

$$DBA3 = e_2 \cos \phi_o [Tempb \; Z_w - Tempc]$$

$$DBA4 = e_2 \cos \phi_o \; Z_w \; Tempc$$

$$DBC1 = -\cos \phi_o e_5 e_1 [L_{\dot{\beta}} M_{\dot{\alpha}} + M_{\dot{\alpha}} N_{\dot{\beta}} (I_{xz}/I_{xx})]$$

$$DBC2 = -\cos \phi_o e_5 e_1 [M_{\dot{\alpha}} L_\beta + e_{14} L_{\dot{\beta}} M_{\dot{\alpha}} + M_\alpha L_{\dot{\beta}} + M_{\dot{\alpha}} N_\beta (I_{xz}/I_{xx})$$
$$- M_{\dot{\alpha}} e_9 N_{\dot{\beta}} + M_\alpha N_{\dot{\beta}} (I_{xz}/I_{xx}) - L_{\dot{\alpha}} N_{\dot{\beta}} e_{11} + N_{\dot{\alpha}} L_{\dot{\beta}} e_{11}]$$

$$DBC3 = -\cos \phi_o e_5 e_1 [M_{\dot{\alpha}} e_{14} L_\beta + M_\alpha L_\beta + M_\alpha e_{14} L_{\dot{\beta}} - M_{\dot{\alpha}} e_9 N_\beta + M_\alpha N_\beta (I_{xz}/I_{xx})$$
$$- M_\alpha e_9 N_\beta - L_{\dot{\alpha}} N_\beta e_{11} + N_{\dot{\alpha}} L_\beta e_{11}]$$

$$DBC4 = \cos \phi_o e_5 e_1 (-M_\alpha e_{14} L_\beta + M_\alpha e_9 N_\beta)$$

50

$$DBD1 = \cos \phi_o e_5 e_3 [M_{\dot\alpha} L_{\dot\beta}(I_{xz}/I_{zz}) + M_{\dot\alpha} N_{\dot\beta}]$$

$$DBD2 = \cos \phi_o e_5 e_3 [M_{\dot\alpha} L_\beta(I_{xz}/I_{zz}) - M_{\dot\alpha} e_{12} L_{\dot\beta} + M_\alpha L_{\dot\beta}(I_{xz}/I_{zz}) + M_\alpha N_{\dot\beta} + M_{\dot\alpha} N_\beta$$
$$- e_7 M_{\dot\alpha} N_{\dot\beta} - e_{10} L_{\dot\alpha} N_{\dot\beta} + e_{10} N_{\dot\alpha} L_{\dot\beta}]$$

$$DBD3 = \cos \phi_o e_5 e_3 [- M_\alpha L_{\dot\beta} e_{12} + M_\alpha L_\beta(I_{xz}/I_{zz}) - M_\alpha e_{12} L_{\dot\beta} + M_\alpha N_\beta - e_7 M_\alpha N_{\dot\beta}$$
$$- e_7 M_{\dot\alpha} N_\beta - e_{10} L_{\dot\alpha} N_\beta + e_{10} N_{\dot\alpha} L_{\dot\beta}]$$

$$DBD4 = \cos \phi_o e_5 e_3 (-M_\alpha N_\beta e_7 - M_\alpha L_\beta e_{12})$$

$$DBF1 = L_\beta(I_{xz}/I_{zz}) + N_{\dot\beta}$$

$$DBF2 = L_{\dot\beta} e_{12} + L_\beta M_q(I_{xz}/I_{zz}) - L_\beta(I_{xz}/I_{zz}) + N_{\dot\beta} e_7 + N_{\dot\beta} M_q - N_\beta$$

$$DBF3 = L_{\dot\beta} e_{10} e_{13} + L_{\dot\beta} e_{12} M_q - L_\beta e_{12} - L_\beta M_q(I_{xz}/I_{zz}) + N_{\dot\beta} e_7 M_q$$
$$- N_\beta e_7 - N_\beta M_q - N_{\dot\beta} e_{10} e_8$$

$$DBF4 = L_\beta e_{10} e_{13} + L_\beta e_{12} M_q + N_\beta e_7 M_q - N_\beta e_{10} e_8$$

$$DBG1 = -\sin \phi_o e_2 [M_{\dot\alpha} L_{\dot\beta}(I_{xz}/I_{zz}) + M_{\dot\alpha} N_{\dot\beta}]$$

$$DBG2 = -\sin \phi_o e_2 [M_\alpha L_\beta(I_{xz}/I_{zz}) - M_\alpha e_{12} L_{\dot\beta} + M_\alpha L_{\dot\beta}(I_{xz}/I_{zz}) + M_\alpha N_\beta - M_{\dot\alpha} e_7 N_\beta$$
$$+ N_{\dot\beta} M_\alpha - L_\alpha N_\beta e_{10} + N_\alpha L_{\dot\beta} e_{10}]$$

$$DBG3 = \sin \phi e_2 [M_{\dot\alpha} e_{12} L_\beta - M_\alpha L_\beta(I_{xz}/I_{zz}) + M_\alpha e_{12} L_{\dot\beta} - M_\alpha e_7 N_\beta - M_\alpha N_\beta$$
$$+ M_\alpha e_7 N_{\dot\beta} + L_{\dot\alpha} N_\beta e_{10} - N_{\dot\alpha} L_\beta e_{10}]$$

$$DBG4 = \sin \phi_o e_2 (M_\alpha e_{12} L_\beta + M_\alpha e_7 N_\beta)$$

$$DBH1 = -(I_{xz}/I_{zz}) L_{\dot\alpha} - N_{\dot\alpha}$$

$$DBH2 = L_\alpha e_{12} + L_{\dot\alpha} M_q(I_{xz}/I_{zz}) + M_\alpha e_{13} + e_7 N_{\dot\alpha} + M_q N_{\dot\alpha} + M_{\dot\alpha}(I_{xz}/I_{zz}) e_8$$

$$DBH3 = -L_{\dot\alpha} e_{10} e_{13} - L_{\dot\alpha} e_{12} M_q - M_\alpha e_{13} e_7 + M_\alpha e_{13} - e_7 M_q N_\alpha + M_\alpha(I_{xz}/I_{zz}) e_8$$
$$- M_\alpha e_{12} e_8 + e_8 N_{\dot\alpha} e_{10}$$

$$DBH4 = M_\alpha e_7 e_{13} + M_\alpha e_{12} e_8$$

$$DBI1 = -\sin\phi_o e_5 e_1 (L_{\dot\alpha} N_{\dot\beta} - L_{\dot\beta} N_{\dot\alpha})$$

$$DBI2 = -\sin\phi_o e_5 e_1 (M_{\dot\alpha} L_{\dot\beta} e_{13} - M_{\dot\alpha} N_{\dot\beta} e_8 + N_{\beta} L_{\dot\alpha} - L_{\dot\alpha} M_q N_{\dot\beta}$$
$$-L_{\beta} N_{\dot\alpha} + M_q L_{\dot\beta} N_{\dot\alpha})$$

$$DBI3 = -\sin\phi_o e_5 e_1 (M_{\alpha} L_{\dot\beta} e_{13} + L_{\beta} M_{\dot\alpha} e_{13} - M_{\alpha} N_{\dot\beta} e_8 - M_{\dot\alpha} N_{\beta} e_8$$
$$- L_{\dot\alpha} M_q N_{\beta} + M_q L_{\beta} N_{\dot\alpha})$$

$$DBI4 = -\sin\phi_o e_5 e_1 (M_{\alpha} L_{\beta} e_{13} - M_{\alpha} N_{\beta} e_8)$$

Static Aerodynamic Coefficients: Body Axis

C_N = Normal force/$\bar{q}S$

C_Y = Side force/$\bar{q}S$

C_A = Axial force/$\bar{q}S$

C_ℓ = Rolling moment/$\bar{q}Sb$

C_m = Pitching moment/$\bar{q}Sc$

C_n = Yawing moment/$\bar{q}Sb$

Static Stability Derivatives: Body Axis, per radian

$C_{N_\alpha} = \partial C_N/\partial\alpha$

$C_{Y_\beta} = \partial C_Y/\partial\beta$

$C_{\ell_\beta} = \partial C_\ell/\partial\beta$

$C_{m_\alpha} = \partial C_m/\partial\alpha$

$C_{n_\beta} = \partial C_n/\partial\beta$

Dynamic Stability Derivatives: Body Axis

$C_{Y_p} = \partial C_Y/\partial(pb/2V_\infty)$

$C_{Y_r} = \partial C_Y/\partial(rb/2V_\infty)$

$C_{\ell_p} = \partial C_\ell/\partial(pb/2V_\infty)$

$C_{\ell_q} = \partial C_\ell/\partial(qc/2V_\infty)$

$C_{\ell_{\dot\beta}} = \partial C_\ell/\partial(\dot\beta b/2V_\infty)$

$C_{\ell_{\dot\alpha}} = \partial C_\ell/\partial(\dot\alpha c/2V_\infty)$

$C_{\ell_r} = \partial C_\ell/\partial(rb/2V_\infty)$

$C_{m_q} = \partial C_m/\partial(qc/2V_\infty)$

$C_{m_r} = \partial C_m/\partial(rb/2V_\infty)$

$C_{m_p} = \partial C_m/\partial(pb/2V_\infty)$

$C_{m_{\dot\alpha}} = \partial C_m/\partial(\dot\alpha b/2V_\infty)$

$C_{n_r} = \partial C_n/\partial(rb/2V_\infty)$

$C_{n_{\dot\beta}} = \partial C_n/\partial(\dot\beta b/2V_\infty)$

$C_{n_{\dot\alpha}} = \partial C_n/\partial(\dot\alpha c/2V_\infty)$

$C_{n_q} = \partial C_n/\partial(qc/2V_\infty)$

$C_{n_p} = \partial C_n/\partial(pb/2V_\infty)$

Dimensional Stability Derivatives: Body Axis

$$L_r = (\rho V_\infty Sb^2/4I_{xy})C_{\ell_r}$$

$$L_v = (\rho V_\infty Sb/2I_{xy})C_{\ell_\beta}$$

$$L_p = (\rho V_\infty Sb^2/4I_{xx})C_{\ell_p}$$

$$L_{\dot{v}} = (\rho Sb^2/4I_{xx})C_{\ell_{\dot\beta}}$$

$$L_q = (\rho V_\infty Sb^2/4I_{xy})C_{\ell_q}$$

$$L_{\dot{w}} = (\rho Sb^2/4I_{xx}\cos\alpha_o)C_{\ell_{\dot\alpha}}$$

$$L_{\dot\alpha} = U_o L_{\dot{w}}$$

$$L_{\dot\beta} = V_\infty L_{\dot{v}}$$

$$L_\beta = V_\infty L_v$$

$$M_w = (\rho V_\infty Sc/2I_{yy}\cos\alpha_o)C_{m_\alpha}$$

$$M_{\dot{w}} = (\rho Sc^2/4I_{yy}\cos\alpha_o)C_{m_{\dot\alpha}}$$

$$M_q = (\rho V_\infty Sc^2/4I_{yy})C_{m_q}$$

$$M_p = (\rho V_\infty Sc^2/4I_{yy})C_{m_p}$$

$$M_r = (\rho V_\infty Sc^2/4I_{yy})C_{m_r}$$

$$M_{\dot\alpha} = U_o M_w$$

$$M_\alpha = U_o M_w$$

$$N_v = (\rho V_\infty Sb/2I_{zz})C_{n_\beta}$$

$$N_{\dot{v}} = (\rho Sb^2/4I_{zz})C_{n_{\dot\beta}}$$

$$N_p = (\rho V_\infty Sb^2/4I_{zz})C_{n_p}$$

$$N_r = (\rho V_\infty Sb^2/4I_{zz})C_{n_r}$$

$$N_{\dot{w}} = (\rho Sb^2/4I_{zz}\cos\alpha_o)C_{n_{\dot\alpha}}$$

$$N_q = (\rho V_\infty Sb^2/4I_{zz})C_{n_q}$$

$$N_{\dot\alpha} = U_o N_{\dot{w}}$$

$$N_{\dot\beta} = V_\infty N_{\dot{v}}$$

$$N_\beta = V_\infty N_v$$

$$Y_v = (\rho V_\infty S/2m)C_{Y_\beta}$$

$$Y_r = (\rho V_\infty Sb/4m)C_{Y_r}$$

$$Y_p = (\rho V_\infty Sb/4m)C_{Y_p}$$

$$-Z_w = (-\rho V_\infty S/2m\cos\alpha_o)(C_{m_\alpha} + C_A)$$

NOMENCLATURE

b	Wing span, ft
c	Wing chord, ft
cg	Aircraft center of gravity
g	Acceleration due to gravity, ft/sec^2
I_{xx}, I_{yy}, I_{zz}	Moments of inertia, body axis, slug-ft^2
I_{xz}	Product of inertia, body axis, slug-ft^2
i_t	Aircraft horizontal stabilizer incidence, deg
m	Aircraft mass, slug
n	Aircraft load factor
p, q, r	Roll, pitch, and yaw rates about aircraft X, Y, and Z body axes
$\dot{p}, \dot{q}, \dot{r}$	Roll, pitch, and yaw accelerations about X, Y, and Z body axes, rad/sec
$\bar{q}$	Dynamic pressure, lb/ft^2
S	Wing area, ft^2
U	Velocity along body X-axis, ft/sec
V_∞	Free-stream velocity, ft/sec
X, Y, Z,	Orthogonal body-axis system fixed in the aircraft with the X-axis along the longitudinal centerline of the body, the Y-axis normal to the plane of symmetry, and the Z-axis in the plane of symmetry

SUBSCRIPTS

α	Aircraft angle of attack, deg
β	Aircraft angle of sideslip, deg
ρ	Aircraft density, slugs/ft^3
ϕ	Aircraft angle of roll